DFG-Schwerpunktprogramm 1324

„Extraktion quantifizierbarer Information aus komplexen Systemen"

Inversion of the noisy Radon transform on $SO(3)$ by Gabor frames and sparse recovery principles

P. Cerejeiras, M. Ferreira, U. Kähler, G. Teschke

Preprint 35

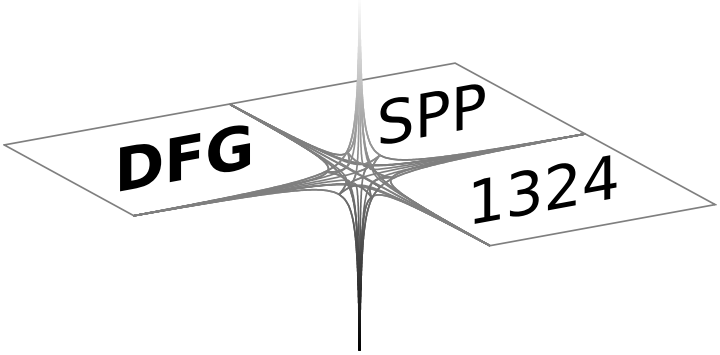

Edited by

AG Numerik/Optimierung
Fachbereich 12 - Mathematik und Informatik
Philipps-Universität Marburg
Hans-Meerwein-Str.
35032 Marburg

DFG-Schwerpunktprogramm 1324

„Extraktion quantifizierbarer Information aus komplexen Systemen"

Inversion of the noisy Radon transform on $SO(3)$ by Gabor frames and sparse recovery principles

P. Cerejeiras, M. Ferreira, U. Kähler, G. Teschke

Preprint 35

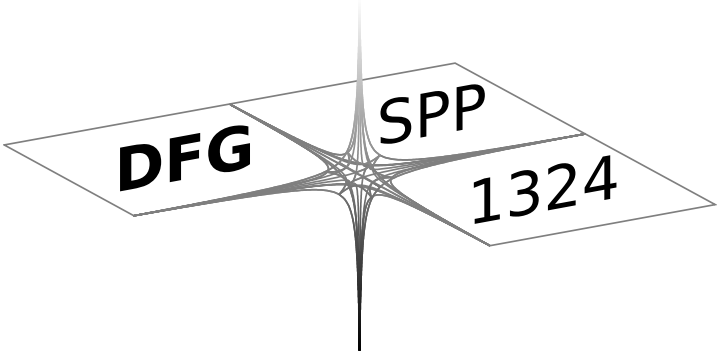

The consecutive numbering of the publications is determined by their chronological order.

The aim of this preprint series is to make new research rapidly available for scientific discussion. Therefore, the responsibility for the contents is solely due to the authors. The publications will be distributed by the authors.

Inversion of the noisy Radon transform on $SO(3)$ by Gabor frames and sparse recovery principles

Paula Cerejeiras* Milton Ferreira† Uwe Kähler* Gerd Teschke‡

Abstract

The inversion of the one-dimensional Radon transform on the rotation group $SO(3)$ is an ill-posed inverse problem that can be applied to X-ray tomography with polycrystalline materials. This paper is concerned with the development of a method to stably approximate the inverse of the noisy Radon transform on $SO(3)$. The proposed approach is composed by basic building blocks of the coorbit theory on homogeneous spaces, Gabor frame constructions and variational principles for sparse recovery. The performance of the finally obtained iterative approximation is studied through several experiments.

Keywords: Radon transform on $SO(3)$, X-ray tomography, Gabor frames, coorbit theory, sparse recovery, crystallography

1 Introduction

The Radon transform on $SO(3)$ becomes an instrument in crystallographic texture analysis as it relates the crystallographic orientation density function (ODF) and its experimentally accessible pole density functions (PDFs), see [25, 4]. Therefore, the determination of a suitable ODF from pole intensity data can be done through the inversion of the Radon transform on $SO(3)$. Several inversion methods (mostly ad hoc procedures) have been studied in the past, see e.g. [5, 17, 18, 24]. To our knowledge an important contribution with mathematical rigor in this field was given by [16] in which a Fourier slice theorem for the Radon transform on SO(3) characterizing the Radon transform as a multiplication operator in Fourier space was elaborated. The authors of [16] present a fast algorithm for the evaluation of the discrete inverse Radon transform in $SO(3)$ based on fast Fourier techniques on the two-dimensional sphere S^2 and the rotational group $SO(3)$.

The procedure presented in this paper is completely different and goes as follows. We consider the Radon transform R as a map between $L_2(S^3)$ and $L_2(S^2 \times S^2)$ (which is in this

*University of Aveiro, Department of Mathematics, 3810-193 Aveiro, Portugal.

†ESTG - Polytechnical Institute of Leiria, Department of Mathematics, 2411-901 Leiria, Portugal.

‡Neubrandenburg University of Applied Sciences, Institute for Computational Mathematics in Science and Technology, Brodaer Str. 2, 17033 Neubrandenburg, Germany

setting an ill-posed operator). To numerically compute an approximation to the solution of the inverse problem $Rf = g$, we have to establish a suitable and reasonable expansion for f. Assuming sparsely localized orientation density functions (and also hoping to achieve some technical operability), we focus on Gabor system expansions for $L_2(S^3)$. This also allows us to work with a spherical grid (becoming the translates) of the window function, which is given in terms of the binary icosahedral group (given by the vertices of the 600-cell). Such a distribution seems to us suitably adapted to the study of ODF's which are invariant under a certain point group (subgroup of the orthogonal group) determined by the crystal under study. In order to establish such a localized Fourier system on S^3, we shall involve the machinery of group representation theory. The construction of associated function spaces and suitable discretizations in them (i.e. the construction of frames) requires a certain concept of function spaces. Here we shall rely on the coorbit theory as it was developed in [8, 7]. With these concepts at hand, we then address the problem of computing an approximate solution of the linear inverse problem. Unfortunately, the function g is in many practical situations not exactly given but only a noisy version g^δ of g with $\|g - g^\delta\| \leq \delta$ is available. Consequently, due to the ill-posedness of R we are therefore faced with regularization issues. To stabilize the inversion process, we propose an iterative procedure that will emerge by the minimization of a residual based variational formulation of the inversion problem. This variational formulation also involves some sparsity constraints leading to thrifty expansions of the ODF. The minimization procedure is close to techniques that were proposed [11, 12, 13, 26] and [9, 27].

The organization of the paper is as follows. In Section 2 we establish the analytical framework that seems to be well-suited for the problem of inverting the Radon transform on $SO(3)$. In particular, we define the Gabor transform, its admissibility, corresponding coorbit spaces, atomic decompositions and frames. In Section 3 we focus on the problem of stably approximating the inverse of the Radon transform on $SO(3)$. Due to the curse of dimensionality, we discuss very efficient approximation techniques as well as thrifty strategies for the computation of the stiffness matrix entries. The section is closed by solving several christallographic problems (synthetic examples). The Annex contains material on the algebra of quaternions.

2 Preliminaries and analytical framework

Within this section we setup the analytical framework from which we assume that is suited for our problem of inverting the Radon transform on $SO(3)$. We start by introducing a group theoretical signal analysis approach, namely the Gabor transform on $SO(3)$, and verify by classical techniques that this transform acts isometrically between $L_2(S^3)$ and $L_2(Spin(4) \times \mathbb{R}^3)$. Due to nice localization properties the Gabor transform is well suited for expanding localized functions on $L_2(S^3)$. In order to construct Gabor systems on $L_2(S^3)$, we briefly review the concept of coorbit theory on homogeneous spaces that was developed in [7, 8]. The coorbit theory was primarily designed to describe the much broader concept of Banach spaces on the basis of square integrable group representations. But even the restriction to Hilbert spaces is very helpful for our purposes as it furnishes the underlying

function space $L_2(S^3)$ with frames for adequately expanding the functions. Proceeding this way we have ansatz systems at our disposal that allow sparse representations (efficient through localization) of ODF functions that we aim to recover and feasible discretizations of the Radon transform operator.

2.1 Gabor transform on $L_2(SO(3))$

In order to establish Gabor analysis for the Hilbert space $L_2(SO(3))$, we first have to identify a suitable phase space G (substitute to the Weyl-Heisenberg group) for the Gabor transform on $L_2(SO(3))$. To relate the Gabor transform image space $L_2(G)$ with $L_2(SO(3))$, we need to construct a group representation of G into the group of unitary operators on $L_2(SO(3))$. This group representation should be preferably square integrable ensuring that the associated Gabor transform is an isometry between $L_2(SO(3))$ and $L_2(G)$.

Let us first find a suitable charaterization of $SO(3)$. There are many coordinate systems and set of parameters for describing the set of rotations in $\mathbb{R}^3$. The coordinate system is typically chosen in dependance on the underlying application. For our purpose, we consider instead of $SO(3)$ its double covering group $Spin(3)$, which is diffeomorphic to the simplectic group $Sp(1)$ of the unit quaternions (3−sphere). For details we refer to the Annex A.2. With this description, we can now follow the ideas of Torrésani, see [28], and construct a version of the windowed Fourier transform on the sphere. Since the usual Fourier transform is generated by translations and modulations, we need similar transformations on the sphere. A natural candidate is the Euclidean group $G := E(4) = Spin(4) \ltimes \mathbb{R}^4$. The group operation in G reads as

$$(s_1, p_1) \circ (s_2, p_2) = (s_1 s_2, p_1 + s_1 p_2 \overline{s_1}) \tag{1}$$

and the inverse element of (s_1, p_1) is

$$(s_1, p_1)^{-1} = (\overline{s_1}, -\overline{s_1} p_1 s_1), \tag{2}$$

where $\overline{s_1}$ denotes the conjugate element of $s_1 \in \mathrm{Spin}(4)$ (see [14]). As a natural analogue to the Schrödinger representation of the Weyl-Heisenberg group on $L_2(\mathbb{R}^n)$, we can define the representation of G on $L^2(S^3)$:

$$U(s,p)f(q) \quad := \quad e^{i\langle p,q\rangle} f\left(\overline{s} q s\right)$$

with $q \in S^3$. Recall that a unitary representation of a locally compact group G on a Hilbert space is a homomorphism U from G into the group of unitary operators $\mathcal{U}(L_2(S^3))$ on $L_2(S^3)$ which is continuous with respect to the strong operator topology. It is easy to check that U is a homomorphism,

$$\begin{aligned} U(s_1,p_1)\left[U(s_2,p_2)f(q)\right] &= U(s_1,p_1)\left[e^{i\langle p_2,q\rangle} f(\overline{s_2} q s_2)\right] \\ &= e^{i\langle p_1,q\rangle} e^{i\langle p_2,\overline{s_1} q s_1\rangle} f(\overline{s_2}\,\overline{s_1} q s_1 s_2) \\ &= e^{i\langle p_1 + s_1 p_2 \overline{s_1},q\rangle} f(\overline{s_1 s_2} q s_1 s_2) \\ &= U((s_1,p_1)\circ(s_2,p_2))f(q). \end{aligned}$$

As already mentioned is [28], this representation is not square-integrable. To overcome this integrability problem we have to consider U restricted to suitably chosen subgroup H of G. One natural candidate for H is given by the stability group $H = \{(0,(0,0,0,p_4)) \in G : p_4 \in \mathbb{R}\}$ of G. The following constructions substantially depend on the choice of the section σ of the principal bundle $\Pi : G \to G/H$. We chose the flat section $\sigma(s,p)$ with $p = (\underline{p},0)$, where $\underline{p} = (p_1,p_2,p_3) \in \mathbb{R}^3$, which is sufficient for our purpose. Then, $X = G/H$ carries the $G-$invariant measure $d\mu(x) = d\mu(s_x)dp_x$, where $x = (s_x,p_x)$. It remains to verify that U is indeed strictly square integrable modulo (U,σ). Therefore, we have to prove that there exists a window functions $\psi \in L^1(S^3)$ such that

$$\begin{aligned} V_\psi f(s,p) &= \langle f, U(\sigma(s,p)^{-1})\psi\rangle & (3)\\ &= \int_{S^3} \overline{e^{-i\langle \overline{s}ps,q\rangle}\overline{\psi}}(sq\overline{s})f(q)dS_q \\ &= \int_{S^3} e^{i\langle p,sq\overline{s}\rangle}\overline{\psi}(sq\overline{s})f(q)dS_q & (4)\end{aligned}$$

is an isometry. This can be shown by applying techniques of [8, 28].

Lemma 1 (admissibility and isometry) *Assume that the window $\psi \in L_1(S^3)\cap L_2(S^3)$ is such that $supp(\psi) \subseteq S^3_+ = \{q \in \mathbb{H} : ||q|| = 1 \wedge q_0 > 0\}$, where q_0 denotes the real part of the unit quaternion q (see Annex A.1),*

$$0 \neq C_\psi = 64\pi^5 \int_0^{2\pi}\int_0^{\pi}\int_0^{\pi/2} \frac{|\psi(q(\theta,\alpha,\phi))|^2}{\cos\phi}\, d\phi\, d\alpha\, d\theta < \infty. \quad (5)$$

Then the map

$$f \in L^2(S^3) \mapsto \frac{1}{\sqrt{C_\psi}} V_\psi f \in L^2(Spin(4)\times\mathbb{R}^3)$$

is an isometry, i.e.

$$\int_{Spin(4)\times\mathbb{R}^3} |V_\psi f(s,p)|^2\, d\mu(s)\, dp = C_\psi \int_{S^3} |f(q)|^2 dS_q.$$

Proof: By a simple substitution we obtain

$$\begin{aligned} ||V_\psi f||^2 &= \int_{Spin(4)}\int_{\mathbb{R}^3} \left| \int_{S^3} e^{i\langle p,sq\overline{s}\rangle}\overline{\psi}(sq\overline{s})f(q)dS_q \right|^2 dp\, d\mu(s) \\ &= \int_{Spin(4)}\int_{\mathbb{R}^3} \left| \int_{S^3} e^{i\langle p,q\rangle}\overline{\psi}(q)f(\overline{s}qs)dS_q \right|^2 dp\, d\mu(s).\end{aligned}$$

Let $q = \Lambda(\theta,\alpha,\phi)$, $\theta \in [0,2\pi[$, $\alpha \in [0,\pi[$ and $\phi \in [0,\pi[$, where Λ denotes the map from spherical to cartesian coordinates defined by

$$\Lambda(\theta,\alpha,\phi) = \begin{cases} q_0 &= \cos\phi \\ q_1 &= \cos\alpha\sin\phi \\ q_2 &= \sin\theta\sin\alpha\sin\phi \\ q_3 &= \cos\theta\sin\alpha\sin\phi \end{cases}. \quad (6)$$

Let also $v : S^3_+ \to B^3$ denote the projection map from the upper hemisphere S^3_+ onto the unit ball B^3 (in $\mathbb{R}^3$) obtained by the change of variable $t = \sin\phi$ in (6) and cutting the real component q_0. Consequently,

$$\begin{aligned}
& \int_{S^3} e^{i\langle p,q\rangle}\overline{\psi}(q) f(\overline{s}qs) dS_q \\
= & \int_{B^3} e^{i\langle x(t,\theta,\alpha),\underline{p}\rangle}\overline{\psi}(v^{-1}(x(t,\theta,\alpha)))f(\overline{s}v^{-1}(x(t,\theta,\alpha))s)\frac{dt}{\sqrt{1-t^2}}d\theta\, d\alpha \\
= & \mathcal{F}\left(\frac{\overline{\psi}(v^{-1}(\cdot))}{\sqrt{1-t^2}} f(\overline{s}v^{-1}(\cdot)s)\right)(\underline{p}),
\end{aligned}$$

where $\underline{p} = (p_1, p_2, p_3)$, and $\mathcal{F}$ denotes the Fourier transform on $\mathbb{R}^3$. Applying Plancherel's Theorem yields

$$\left\|\mathcal{F}\left(\frac{\overline{\psi}(v^{-1}(\cdot))}{\sqrt{1-t^2}} f(\overline{s}v^{-1}(\cdot)s)\right)\right\|^2_{L^2(\mathbb{R}^3)} = (2\pi)^3 \left\|\frac{\overline{\psi}(v^{-1}(\cdot))}{\sqrt{1-t^2}} f(\overline{s}v^{-1}(\cdot)s)\right\|^2_{L^2(B^3)}.$$

Returning to the unit sphere S^3 by setting $\phi = \arcsin t$, we obtain

$$||V_\psi f||^2 = 8\pi^3 \int_{\mathrm{Spin}(4)} \int_{S^3_+} \frac{|\overline{\psi}(\Lambda(\theta,\alpha,\phi))|^2}{\cos\phi} |f(\overline{s}\Lambda(\theta,\alpha,\phi)s)|^2 \, d\phi\, d\alpha\, d\theta\, d\mu(s).$$

By Fubini's theorem and using the invariance of the measures $d\mu(s)$ (see [28]) we get

$$\begin{aligned}
||V_\psi f||^2 &= 8\pi^3 \int_{S^3_+} \frac{|\overline{\psi}(\Lambda(\theta,\alpha,\phi))|^2}{\cos\phi} \int_{\mathrm{Spin}(4)} |f(\overline{s}\Lambda(\theta,\alpha,\phi)s)|^2 \, d\mu(s)\, d\phi\, d\alpha\, d\theta \\
&= 8\pi^3 \int_{S^3_+} \frac{|\overline{\psi}(\Lambda(\theta,\alpha,\phi))|^2}{\cos\phi} 8\pi^2 ||f||^2_{L^2(S^3)}\, d\phi\, d\alpha\, d\theta \\
&= 64\pi^5 \int_{S^3_+} \frac{|\overline{\psi}(\Lambda(\theta,\alpha,\phi))|^2}{\cos\phi}\, d\phi\, d\alpha\, d\theta\, ||f||^2_{L^2(S^3)}.
\end{aligned}$$

■

If ψ fulfills (5), then ψ is called *admissible* with respect to σ. In this case, (ψ, σ) is called a *strictly admissible pair*.

As a consequence, the proposed windowed Fourier transform can be inverted by its adjoint $V^*_\psi/\sqrt{C_\psi}$.

Corollary 1 (reconstruction) *Any $f \in L^2(S^3)$ can be reconstructed by*

$$f(q) = \frac{1}{C_\psi} \int_{Spin(4)} \int_{\mathbb{R}^3} V_\psi f(s,p) e^{-i\langle \overline{s}ps, q\rangle} \psi(sq\overline{s})\, dp\, d\mu(s).$$

2.2 Reproducing kernel Hilbert space and frame theory

To keep notations and technicalities of the coorbit space theory at some reasonable level, we only sketch the main ingredients and review the main conditions that need to be verified for our specific situation.

Assume that (ψ, σ) is a strictly admissible pair. In order to establish frames in $L_2(S^3)$, the coorbit theory restricted to Hilbert spaces suggests the following proceeding. We first have to establish a correspondence principle between $L_2(S^3)$ and an associated reproducing kernel Hilbert space (as a subspace of $L_2(Spin(4) \times \mathbb{R}^3)$). Then a suitable discretization $\{x_i\}_{i\in I} \subset Spin(4) \times \mathbb{R}^3$ must be chosen that enables the derivation of frames.

Let us define the kernel function

$$R(l,h) \quad = \quad \langle \psi, U(\sigma(h)\sigma(l)^{-1})\psi \rangle = V_\psi(U(\sigma(l)^{-1})\psi)(h)$$

and the reproducing kernel Hilbert space

$$\mathcal{M}_2 := \{F \in L_2(Spin(4) \times \mathbb{R}^3) : \ \langle F, R(h,\cdot)\rangle = F\} \ .$$

The following correspondence principle holds true, see [8].

Proposition 1 (correspondence principle) *Let U be a square integrable representation of the Euclidean group $Spin(4) \ltimes \mathbb{R}^4$ mod (H, σ) with a strictly admissible pair (ψ, σ). Then V_ψ is a bijection of $L_2(S^3)$ onto the reproducing kernel Hilbert space $\mathcal{M}_2$.*

The next step is to derive frames for this space. The major tool in [7, 8] is the construction of a bounded partition of unity corresponding to some $\mathcal{U}$-dense and relatively separated sequence $\{x_i\}_{i\in I} \subset X$ that represents then our desired discretization. A sequence $\{x_i\}_{i\in I}$ is called *$\mathcal{U}$-dense* if $\bigcup_{i\in I} \sigma(x_i)\mathcal{U} \supset \sigma(X)$ for some relatively compact neighbourhood $\mathcal{U}$ of the identity $e \in Spin(4) \ltimes \mathbb{R}^3$ with non-void interior and is called *relatively separated*, if $\sup_{j\in I} \sharp\{i \in I : \sigma(x_i)L \cap \sigma(x_j)L \neq \emptyset\} \leq C_L$ for all compact subsets $L \subset Spin(4) \times \mathbb{R}^3$. It can be proved that there always exist such sequences $\{x_i\}_{i\in I}$ for all locally compact groups, all closed subspaces H and all relatively compact neighbourhoods $\mathcal{U}$ of e with non-void interior. Note that the subsets $X_i := \{x \in X : \sigma(x) \in \sigma(x_i)\mathcal{U}\}$ clearly form a covering of X with uniformly finite overlap.

In [7] a judicious discretization for the rotations/translations was suggested due to an Euler angle parametrization of the sphere (but no specific choice was made, just conditions were verified). In there, the discrete frequencies were obtained by a straightforward uniform spacing of the Euclidean space. However, in the present case of $Spin(4)$ that would imply dealing with 6 parameters. Due to the high computational cost involved one is forced to implement a reduction of our parameter space to $Spin(3) \equiv S^3$. This reduction will be described in the next section.

In this paper, we propose to obtain a translation grid by applying a direct spherical discretization method that was elaborated in [21]. This method yields a 'fair' grid, i.e., a near-uniformly spaced spherical grid (up to certain precision of the uniform spacing). To obtain the spherical grid points, a subdivision scheme is developed that is based on the spherical kinematic mapping. This goes as follows: In a first step an elliptic linear

congruence is discretized by the icosahedral discretization of the unit sphere S^3. Then the resulting lines of the elliptic three-space are discretized such that the difference between the maximal and minimal elliptic distance between neighbouring grid points becomes minimal.

Assume the grid is chosen as mentioned above and fulfills the requirements. Then the problem arises under which conditions a function f has an atomic decomposition and the set $\{U(\sigma(x_i))\psi : i \in I\}$ forms a frame. To answer this question, we have to define the $\mathrm{osc}_{\mathcal{U}}$ kernel

$$\mathrm{osc}_{\mathcal{U}}(l,h) := \sup_{u\in\mathcal{U}} \left|\langle \psi, U(\sigma(l)\sigma(h)^{-1})\psi - U(u^{-1}\sigma(l)\sigma(h)^{-1})\psi\rangle_{L_2(S^3)}\right| .$$

On the basis of $\mathrm{osc}_{\mathcal{U}}$ we have the following two major statements at our disposal, see [7, 8].

Theorem 1 (atomic decomposition) *Assume that the relatively compact neighborhood $\mathcal{U}$ of the identity in $Spin(4)\times\mathbb{R}^3$ can be chosen so small such that*

$$\int_X \mathrm{osc}_{\mathcal{U}}(l,h)d\mu(l) < \gamma \quad \textit{and} \quad \int_X \mathrm{osc}_{\mathcal{U}}(l,h)d\mu(h) < \gamma \tag{7}$$

with $\gamma < 1$. Let $\{x_i\}_{i\in I}$ be a $\mathcal{U}$-dense, relatively separated family. Then $L_2(S^3)$ has the following atomic decomposition: if $f \in L_2(S^3)$, then there exists a sequence $c = (c_i)_{i\in I}$ such that f can be represented as

$$f = \sum_{i\in I} c_i U(\sigma(x_i))\psi \ ,$$

where $c \in \ell_2$ and $\|c\|_{\ell_2} \le A\|f\|_{L_2(S^3)}$. If $c \in \ell_2$, then $f = \sum_{i\in I} c_i U(\sigma(x_i))\psi \in L_2(S^3)$ and $\|f\|_{L_2(S^3)} \le B\|c\|_{\ell_2}$.

Theorem 2 (frames) *Impose the same assumptions as in Theorem 1 with*

$$\int_X \mathrm{osc}_{\mathcal{U}}(l,h)d\mu(l) < \frac{\eta}{C_\psi} \quad \textit{and} \quad \int_X \mathrm{osc}_{\mathcal{U}}(l,h)d\mu(h) < \frac{\eta}{C_\psi} \tag{8}$$

with $\eta < 1$. Then the set

$$\{\psi_i := U(\sigma(x_i))\psi : i \in I\}$$

is a frame for $L_2(S^3)$. This means that

1. *$f \in L_2(S^3) \Leftrightarrow \{\langle f, \psi_i\rangle\}_{i\in I} \in \ell_2$,*
2. *there exists constants $0 < A \le B < \infty$ such that*

$$A\|f\|_{L_2(S^3)} \le \|\{\langle f, \psi_i\rangle\}_{i\in I}\|_{\ell_2} \le B\|f\|_{L_2(S^3)} \ ,$$

3. *there exists a bounded, linear synthesis operator $S : \ell_2 \to L_2(S^3)$ such that $S(\{\langle f, \psi_i\rangle\}_{i\in I}) = f$.*

2.3 Verification of frame conditions

In order to establish the statements in Theorems 1 and 2 we have to verify conditions (7) and (8). Before that, to simplify the technicalities and later therewith the computational complexity, we reduce the number of parameters in $X = Spin(4) \times \mathbb{R}^3$ (nine parameters) through restricting ourselves to zonal window functions. Thus, we can consider the factorization of $Spin(4)$ by $Spin(3)$, i.e. $Spin(4)/Spin(3) \simeq S^3$; which allows to to consider $L_2(S^3 \times \mathbb{R}^3)$.

Let us now exemplify by checking condition (7) in Theorem 1. Note that condition (8) in Theorem 2 can be verified analogously and is therefore omitted. Let $h = (s_1, p), l = (s_2, r) \in G/H$ with $p = (p_1, p_2, p_3, 0)$ and $r = (r_1, r_2, r_3, 0)$ be given. Then, by (2) and (1) we have

$$\sigma(h)\sigma(l)^{-1} = (s_1, p) \circ (\overline{s_2}, -\overline{s_2} r s_2) = (s_1 \overline{s_2}, p - s_1 \overline{s_2} r s_2 \overline{s_1}).$$

Let the neighborhood of e be given by $\mathcal{U}_\epsilon := \{u = (s_u, p_u) : s_u \in C_\epsilon,\ p_u \in [-\epsilon, \epsilon]^3\} \subset S^3 \times \mathbb{R}^3$, with $C_\epsilon = \{\Lambda(\theta, \alpha, \phi) : \theta \in [0, 2\pi), \alpha \in [0, \pi), \phi \in [0, \epsilon\pi)\}$ a spherical ϵ-cap. The sampling grid $\{x_i\}_{i \in I}$ can be specified by $x_i = x_{i(m,n)} = (s_m, p_n)$, where the s_m correspond to the grid points generated with the above mentioned algorithm elaborated in [21] and the p_n are uniformly spaced points in $\mathbb{R}^3$. For each chosen ϵ the sampling density can be accordingly adjusted (on S^3 by the subdivision scheme in [21] and in $\mathbb{R}^3$ simply by a finer and finer spacing) such that $X_i = \{x \in X : \sigma(x) \in \sigma(x_i)\mathcal{U}\}$ forms a covering of X that is $\mathcal{U}$-dense and relatively separated. To show that the oscillation condition can be made small enough we proceed similar as in [8]. With the help of

$$\sigma(h)\sigma(l)^{-1} u = (s_1 \overline{s_2} s_u, p - s_1 \overline{s_2}(r - p_u) s_2 \overline{s_1})$$

we obtain

$$\begin{aligned}
& \int_{S^3} (U(\sigma(l)\sigma(h)^{-1})\psi(q)\overline{\psi}(q) - U(\sigma(l)\sigma(h)^{-1}u)\psi(q)\overline{\psi}(q))\, dS_q \\
= & \int_{S^3} (e^{i\langle q, p - s_1\overline{s_2} r s_2 \overline{s_1}\rangle} \psi(s_2\overline{s_1} q s_1 \overline{s_2})\overline{\psi}(q) - e^{i\langle q, p - s_1\overline{s_2}(r - p_u)s_2\overline{s_1}\rangle}\, \psi(s_2\overline{s_1} s_u q \overline{s_u} s_1 \overline{s_2})\overline{\psi}(q))\, dS_q \\
= & \int_{S^3_+} e^{i\langle q, p - s_1\overline{s_2} r s_2 \overline{s_1}\rangle} \left[(\psi(s_2\overline{s_1} q s_1 \overline{s_2}) - \psi(s_2\overline{s_1} s_u q \overline{s_u} s_1 \overline{s_2}))\, \overline{\psi}(q) + \right. \\
& \left. \left(1 - e^{i\langle q, s_1\overline{s_2} p_u s_2 \overline{s_1}\rangle} \psi(s_2\overline{s_1} s_u q \overline{s_u} s_1 \overline{s_2})\overline{\psi}(q)\right)\right]\, dS_q
\end{aligned}$$

leading to

$$\begin{aligned}
\mathrm{osc}_{\mathcal{U}}(l, h) \quad \leq \quad & \sup_{u \in \mathcal{U}} \left| \int_{S^3_+} e^{i\langle q, p - s_1\overline{s_2} r s_2 \overline{s_1}\rangle} \left(\psi(s_2\overline{s_1} q s_1 \overline{s_2}) - \psi(s_2\overline{s_1} s_u q \overline{s_u} s_1 \overline{s_2})\right) \overline{\psi}(q)\, dS_q \right| \\
& + \sup_{u \in \mathcal{U}} \left| \int_{S^3_+} e^{i\langle q, p - s_1\overline{s_2} r s_2 \overline{s_1}\rangle} \left(1 - e^{i\langle q, s_1\overline{s_2} p_u s_2 \overline{s_1}\rangle}\right) \psi(s_2\overline{s_1} s_u q \overline{s_u} s_1 \overline{s_2})\overline{\psi}(q)\, dS_q \right|.
\end{aligned}$$

To bound $I := \int_X \operatorname{osc}_{\mathcal{U}}(l,h)d\mu(h)$ we apply the latter estimate and achieve

$$I \leq \int_{S^3} (I_1 + I_2)\, d\mu(s_1)$$

where

$$I_1 := \int_{\mathbb{R}^3} \sup_{u\in\mathcal{U}} \left| \int_{S^3_+} e^{i\langle q, p - s_1\overline{s_2} r s_2 \overline{s_1}\rangle} \left[\psi(s_2\overline{s_1} q s_1 \overline{s_2}) - \psi(s_2\overline{s_1} s_u q \overline{s_u} s_1 \overline{s_2})\right] \overline{\psi}(q)\, dS_q \right| dp,$$

and

$$I_2 := \int_{\mathbb{R}^3} \sup_{u\in\mathcal{U}} \left| \int_{S^3_+} e^{i\langle q, p - s_1\overline{s_2} r s_2 \overline{s_1}\rangle} \left(1 - e^{i\langle q, s_1\overline{s_2} p_u s_2 \overline{s_1}\rangle}\right) \psi(s_2\overline{s_1} s_u q \overline{s_u} s_1 \overline{s_2}) \overline{\psi}(q)\, dS_q \right| dp.$$

We first consider I_1. Projecting q onto the unit ball B^3 yields

$$\begin{aligned} I_1 := \int_{\mathbb{R}^3} \sup_{u\in\mathcal{U}} \Bigg| \int_{B^3} & e^{i\langle x(t,\theta,\alpha), \underline{p}\rangle} e^{-i\langle x(t,\theta,\alpha), s_1\overline{s_2} r s_2 \overline{s_1}\rangle} \left[\psi(s_2\overline{s_1} v^{-1}(x(t,\theta,\alpha)) s_1 \overline{s_2}) \right. \\ & \left. - \psi(s_2\overline{s_1} s_u v^{-1}(x(t,\theta,\alpha)) \overline{s_u} s_1 \overline{s_2})\right] \overline{\psi}(x(t,\theta,\alpha)) \frac{dt}{\sqrt{1-t^2}}\, d\theta\, d\alpha \Bigg| d\underline{p}. \end{aligned}$$

Introducing the functions

$$g(t,\theta,\alpha) = \begin{cases} \frac{e^{-i\langle x(t,\theta,\alpha), s_1\overline{s_2} r s_2 \overline{s_1}\rangle} \sqrt{\overline{\psi}(x(t,\theta,\alpha))}}{\sqrt{1-t^2}}, & t \in [0,1], \theta \in [-\pi,\pi], \alpha \in [0,\pi[, \\ 0, & \text{otherwise}, \end{cases}$$

and

$$w_{s_u}(t,\theta,\alpha) = \begin{cases} \left[\psi(s_2\overline{s_1} v^{-1}(x(t,\theta,\alpha)) s_1 \overline{s_2}) \right. & t \in [0,1], \theta \in [-\pi,\pi], \alpha \in [0,\pi[, \\ \left. -\psi(s_2\overline{s_1} s_u v^{-1}(x(t,\theta,\alpha)) \overline{s_u} s_1 \overline{s_2})\right] & \\ \times \sqrt{\overline{\psi}(x(t,\theta,\alpha))}, & \\ 0, & \text{otherwise}, \end{cases}$$

we can rewrite I_1 as

$$\begin{aligned} I_1 &= \int_{\mathbb{R}^3} \sup_{u\in\mathcal{U}} \left| \int_{-\infty}^{\infty} \int_0^{\pi} \int_{-\pi}^{\pi} e^{i\langle x(t,\theta,\alpha), \underline{p}\rangle} w_{s_u}(t,\theta,\alpha) g(t,\theta,\alpha)\, d\theta\, d\alpha\, dt \right| d\underline{p} \\ &\leq \int_{\mathbb{R}^3} \sup_{u\in\mathcal{U}} \left| (\mathcal{F}(w_{s_u}) * \mathcal{F}g)(\underline{p}) \right| d\underline{p} \\ &\leq \int_{\mathbb{R}^3} \sup_{u\in\mathcal{U}} \int_{\mathbb{R}^3} |(\mathcal{F}(w_{s_u})(\xi)| |\mathcal{F}g((\underline{p}) - \xi)| d\xi\, d\underline{p}. \end{aligned} \tag{9}$$

Observe that w_{s_u} has compact support. Now, if we choose ψ smooth enough, i.e. $w_{s_u} \in C^k(\mathbb{R}^3), k \geq 4$, and $g \in L_1$, then $\lim_{s_u \to \mathrm{id}} w_{s_u}^{(k)} = 0$ and by dominated convergence we have that

$$\lim_{s_u \to \mathrm{id}} ||w_{s_u}^{(k)}||_{L_1} = 0.$$

This also implies that

$$\lim_{s_u \to \mathrm{id}} ||\mathcal{F}(w_{s_u}^{(k)})||_{L_\infty} = 0.$$

Therefore, by using

$$\mathcal{F}(w_{s_u}^{(k)})(\xi) = (-i\xi)^k \mathcal{F}(w_{s_u})(\xi)$$

we have

$$|\mathcal{F}(w_{s_u}^{(k)})(\xi)| \leq (1+|\xi|)^{-k} c(s_u), \tag{10}$$

where $c(s_u)$ denotes a continuous function with $\lim_{s_u \to \mathrm{id}} c(s_u) = 0$. Inserting (10) into (9), we obtain

$$\begin{aligned} I_2 &\leq \int_{\mathbb{R}^3} \sup_{u \in \mathcal{U}} c(s_u) \int_{\mathbb{R}^3} (1+|\xi|)^{-r} |\mathcal{F}g(\underline{p}-\xi)| d\xi \, d\underline{p} \\ &\leq ||\mathcal{F}(g)||_{L_1} \sup_{s_u \in C_\epsilon} c(s_u) \int_{\mathbb{R}^3} (1+|\xi|)^{-r} d\xi \\ &\leq C \sup_{s_u \in C_\epsilon} c(s_u). \end{aligned}$$

This expression becomes arbitrary small for sufficient small ϵ. The second integral I_2 can be treated in the same way. In this case the function w_{p_u} is given by $\left(1 - e^{i\langle \omega, s_1 \overline{s_2} p_u s_2 \overline{s_1} \rangle}\right) \sqrt{\overline{\psi}(q)}$. Imposing the same regularity condition on ψ as done in the estimate of I_1 one can apply similar arguments.

3 Inversion of the X-ray transform

This section is concerned with the determination of the orientation density function f (ODF) of a polycrystalline specimen from given pole intensity data. The major assumption is that f can be sufficiently well represented by spherical Gabor frames as they were introduced in the previous section. Then the remaining task is to solve a discretized operator equation, i.e., to determine the synthesis coefficients (or the atomic representation) of f. As the data are allowed to be noisy (which is for any practical measurement process impossible to avoid), the Radon or X-ray operator must be considered between $L_2(S^3)$ and $L_2(S^2 \times S^2)$ and is, therefore, ill-posed (and not as the operator properties suggest as a map with negative order between Sobolev spaces (see [3])). Consequently we are therefore faced with regularization issues, i.e., the inversion procedure must be stabilized against the influence of the noise.

3.1 Crystallography and the spherical X-ray transform

The orientation of an individual crystal is assumed to be unique and given by the rotation $q \in SO(3)$ which maps the specimen referential system K_s into coincidence with a coordinate system K_c fixed to the crystal, $q : K_s \mapsto K_c$. Hence the coordinates of the initial direction represented by $x \in S^2 \subset \mathbb{R}^3$ (w.r.t. the crystal coordinate system K_c) will be related to the ones of the final direction represented by $y \in S^2$ (w.r.t. the coordinate system K_s) by $y = \overline{q} x q$. With other words we assume that a crystal is uniquely determined

by its invariance group (crystallographic group) $G \subset O(3) \times T(3)$. We are here interested in the part which corresponds to a subgroup (point group) $G_p := G/T(3) \subset O(3)$. A nonnegative, integrable (possibly normalized) function

$$f : O(3)/G_p \mapsto \mathbb{R}_+$$

is called an orientation density function (ODF). The determination of such an ODF is called quantitative texture analysis. The ODF f can only be measured in an indirect way via the pole density function $\tilde{P}(x,y) = \frac{1}{2}\left((Rf)(x,y) + (Rf)(-x,y)\right)$, there is, by means of two spherical X-ray transforms of the orientation density function f ([25], [6]). The principle problem consists in how to determine the ODF from the measurements (pole figures).

Definition 1 *[Spherical X-ray transform] [6]) Let f be a $L^1(S^3)$ function. We define the spherical X-ray transform of f as the mean over all rotations q mapping the direction $x \in S^2$ into $y \in S^2$ and we write*

$$\begin{aligned}(Rf)(x,y) &:= \frac{1}{2\pi}\int_{\{q\in S^3 : y=\bar{q}xq\}} f(q)dq \\ &= \frac{1}{2\pi}\int_0^{2\pi} f(q(x,y,t))dt,\end{aligned}$$

where $q(x,y,t) = \left(\cos\frac{\eta}{2} + \frac{x\times y}{\|x\times y\|}\sin\frac{\eta}{2}\right)\cos t + \frac{x+y}{\|x+y\|}\sin t$, with $\eta = \arccos(\langle x,y\rangle)$, denotes the great circle in S^3 of all unit quaternions q which rotates $x \in S^2$ into $y \in S^2$.

Note that the invariant Haar measure in (11) is uniquely defined by the assumption that the measurements should be independent of the choices of the coordinate systems K_c, K_s.

3.2 Inversion by accelerated steepest descent and ℓ_1-projections

In this section, we address the problem of computing an approximation to a solution of the linear problem $R(f) = g$, where R denotes the X-ray transform. The operator R is an integral operator and therefore $R(f)$ belongs to a certain smoothness (Sobolev) space. But usually we deal with noisy data g^δ instead of g. Consequently, we only can assume $R : L_2(S^3) \to L_2(S^2 \times S^2)$, at most.

The function f is often referred to as a probabilistic density function on $L_2(S^3)$. In typical practical situations only noisy data g^δ with $\|g - g^\delta\| \leq \delta$ are available. Therefore, we are faced with the problem of ill-posedness (in the sense of a discontinuous dependence of the solution on the data) and therefore with regularization issues.

The goal is to propose an iterative procedure for deriving an approximation to the solution of our inverse problem. To this end, we start by providing an adequate representation of the solution to be reconstructed. Our preference is on a Gabor frame for $L_2(S^3)$ and was established in the previous section. Let Λ be the countable index set representing

the frame grid and let the Gabor frame be denoted by $\Psi = \{\psi_\lambda : \lambda \in \Lambda\} \subset L_2(S^3)$. An individual Gabor atom indexed by the multi-index λ is of the form

$$\psi_\lambda(q) = \psi_{(n,m)}(q) = U(s_n, p_m)\psi(q) = e^{i\langle q, p_m\rangle}\psi(\bar{s}_n q s_n) \ .$$

In this notation n and m are also multi-indices. For Ψ we may consider the operator

$$F : L_2(S^3) \to \ell_2(\Lambda) \quad \text{via} \quad f \mapsto \{\langle f, \psi_\lambda\rangle\}_{\lambda\in\Lambda}$$

with adjoint

$$F^* : \ell_2(\Lambda) \to L_2(S^3) \quad \text{via} \quad c \mapsto \sum_{\lambda\in\Lambda} c_\lambda \psi_\lambda \ .$$

Therefore, the inverse problem can be recast as follows: find a sequence $c \in \ell_2(\Lambda)$ such that

$$R(F^*c) = g.$$

Note that due to the overcompleteness of Ψ, c need not to be unique. Since the data might be inexact (no equality between $R(f)$ and g^δ), we focus on minimizing the Gaussian discrepancy

$$D(c) := \|g^\delta - R(F^*c)\|^2_{L_2(S^2\times S^2)} \ .$$

In this application we can assume that the solution c to be reconstructed has a sparse expansion, i.e. c has only a few nonvanishing coefficients or can be nicely approximated by a small number of coefficients. One well-understood approach to involve this sparsity constraint is given by adding an ℓ_1 penalty term to the Gaussian discrepancy leading to

$$D(c) + \gamma\|c\|_{\ell_1(\Lambda)} \ .$$

The treatment of such functionals is not difficult to handle and was elaborated and successfully applied in several papers, see, e.g., [10, 11, 12, 13, 26]. However, the resulting iteration is known to converge usually quite slow and a detailed analysis of the characteristic dynamics of the corresponding thresholded Landweber iteration has shown that the algorithm converges initially relatively fast, then it overshoots the ℓ_1 penalty, and it takes very long to re-correct back. To circumvent this "external" detour it was proposed in [9, 27] to force the iterates to remain within a particular ℓ_1 ball $B_K := \{x \in \ell_2; \|x\|_{\ell_1(\Lambda)} \le K\}$. This leads to the constrained minimization approach

$$\min_{c\in B_K} D(c) \ . \tag{11}$$

To accelerate the resulting iteration we may apply techniques from standard linear steepest descent methods which is the use of adaptive step lengths. Therefore, a minimization of (11) results in a projected iteration with step length control,

$$c_\lambda^{n+1} = P_K\left(c_\lambda^n + \frac{\beta^n}{r} F R^*(y - R(F^*c^n))\right). \tag{12}$$

The convergence of this method relies on a proper step length parameter rule for β^n. With respect to a sequence $\{c^n\}_{n\in\mathbb{N}}$ the parameter β^n must be chosen such that

$$\text{(B1)} \qquad \bar{\beta} := \sup\{\beta^n; n \in \mathbb{N}\} < \infty \quad \text{and} \quad \inf\{\beta^n; n \in \mathbb{N}\} \geq 1$$
$$\text{(B2)} \qquad \beta^n \|R(F^* c^{n+1}) - R(F^* c^n)\|^2 \leq r \|c^{n+1} - c^n\|^2 \quad \forall n \geq n_0$$

are fulfilled, where the constant r is an upper bound for $\|RF^*\|^2$. Practically, the implementation of the proposed projected steepest descent algorithm is as follows

Given	operator R, some initial guess c^0, and K (sparsity constraint ℓ_1-ball B_K)
Initialization	$\|RF^*\|^2 \leq r$, set $q = 0.9$ (as an example)
Iteration	**for** $n = 0, 1, 2, \ldots$ **until** a preassigned precision / maximum number of iterations **1.** $\beta^n = C \cdot \sqrt{\frac{D(x^0)}{D(x^n)}}$, $C \geq 1$ (greedy guess) **2.** $c^{n+1} = P_K\left(c^n + \frac{\beta^n}{r} FR^*(y - R(F^*(c^n)))\right)$; **3.** verify (B2): $\beta^n \|R(F^* c^{n+1}) - R(F^* c^n)\|^2 \leq r \|c^{n+1} - c^n\|^2$ **if** (B2) is satisfied increase n and go to **1.** **otherwise** set $\beta^n = q \cdot \beta^n$ and go to **2.** **end**

When performing the iteration (12) the main operating expense is due to computation and application of FR^*RF^*. Therefore, an adaptive variant of the full iteration by involving adaptive matrix vector multiplications could significantly reduce the numerical complexity. Unfortunately, the matrix FR^*RF^* belongs neither to the Jaffard nor to the Lemarie class. Therefore, so far established adaptive strategies for operator equations cannot be applied in a straightforward way as done in the Euclidean situation, see [23]. Nevertheless, efficient strategies for computing the matrix entries are possible and allow thrifty linear approximation techniques.

3.3 Efficient computation of matrix entries

In this section we discuss the efficient calculation of the matrix FR^*RF^*. Its entries read as

$$\langle R\psi_{m,n}, R\psi_{m',n'} \rangle_{L_2(S^2 \times S^2)} = \int_{S^2} \int_{S^2} R\psi_{m,n}(x,y) \overline{R\psi_{m',n'}(x,y)} \, dy \, dx. \tag{13}$$

In order to simplify the practical calculations we will consider ψ a zonal window function with support on the spherical cap $U_h = \{q \in S^3 : q_0 \geq h\}$, for some $h \in]0,1[$. As an

immediate consequence the parameter space is reduced to $X = S^3 \times \mathbb{R}^3$ and the action $sq\overline{s}$, $s \in Spin(4)$ can be replaced by the left translation action on S^3 defined by $\overline{s}q$, where $s \in S^3$. This is a left transitive action on S^3 such that the rotations from $Spin(3)$ around a point $q \in S^3$ are left out (see Annex A.2). In this way the X-Ray transform of our atoms is given by

$$R\psi_{m,n}(x,y) = \frac{1}{2\pi}\int_0^{2\pi} e^{i\langle q(x,y,t),p_m\rangle}\psi\left(\overline{s_n}q(x,y,t)\right)dt \ , \tag{14}$$

with $s_n \in S^3$ and $p_m \in \mathbb{R}^3$.

In order to reduce the computational cost of (13) we will look now for symmetry properties of $R\psi_{m,n}$. Since

$$\begin{aligned} R\psi_{m,n}(x,y) &= \frac{1}{2\pi}\int_0^{2\pi} e^{i\langle q(x,y,t),p_m\rangle}\psi\left(\overline{s_n}q(x,y,t)\right)dt & (15)\\ &= \frac{1}{2\pi}\int_{-\pi}^{\pi} e^{i\langle q(x,y,t),p_m\rangle}\psi\left(\overline{s_n}q(x,y,t)\right)dt & (16)\end{aligned}$$

then it is easy to see that $R\psi_{m,n}(-x,-y) = R\psi_{m,n}(x,y)$. Therefore, the inner products (13) reduce to

$$\begin{aligned}\langle R\psi_{m,n}, R\psi_{m',n'}\rangle_{L_2(S^2\times S^2)} &= 2\int_{S^2_+}\int_{S^2_+} R\psi_{m,n}(x,y)\overline{R\psi_{m',n'}(x,y)}\,dy\,dx \\ &\quad +2\int_{S^2_+}\int_{S^2_-} R\psi_{m,n}(x,y)\overline{R\psi_{m',n'}(x,y)}\,dy\,dx \ , \end{aligned}\tag{17}$$

where S^2_+ and S^2_- represents the upper ($x_3 \geq 0$) and lower ($x_3 \leq 0$) hemispheres respectively.

The standard parametrization of great circles of S^3 by $q(x,y,t)$ as given in Definition 1 has a singularity in $y = -x$, that is, if $y = -x$ this parametrization is not well defined. Moreover, the gradient of $q(x,y,t)$ increases rapidly in a neighborhood of $y = -x$. To overcome this problem we will make a reparametrization of the great circles $q(x,y,t)$. By [20] we can reparametrize the great circle $q(x,y,t)$ introducing a vector $v \in S^2$ in the following way:

$$q(x,y,t) = q_4 v(t) q_3 \ , \tag{18}$$

where

i) q_3 is any fixed quaternion such that $q_3 x\overline{q_3} = v$, with an arbitrarily given $v \in S^2$;

ii) $v(t) = \cos t/2 + v\sin t/2 \in S^3$ such that $v(t)v\overline{v(t)} = v$;

iii) $q_4 \in S^3$ is any fixed quaternion such that $q_4 v\overline{q_4} = y$.

Choosing $q_4 = \frac{y+v}{||y+v||}$ and $q_3 = \frac{x+v}{||x+v||}$ the new parametrization (18) is given by

$$q(x,y,t) = \frac{y+v}{||y+v||}\left(\cos t + v\sin t\right)\frac{x+v}{||x+v||}. \tag{19}$$

Thus, we will consider the following integrals:

$$\mathcal{I}_1 = \int_{S^2_+}\int_{S^2_+} R\psi_{m,n}(x,y)\overline{R\psi_{m',n'}(x,y)}\; dy\; dx, \tag{20}$$

$$\mathcal{I}_2 = \int_{S^2_+:x_1\geq 0}\int_{S^2_-} R\psi_{m,n}(x,y)\overline{R\psi_{m',n'}(x,y)}\; dy\; dx, \tag{21}$$

$$\mathcal{I}_3 = \int_{S^2_+:x_1\leq 0}\int_{S^2_-} R\psi_{m,n}(x,y)\overline{R\psi_{m',n'}(x,y)}\; dy\; dx. \tag{22}$$

For each integral we will consider the new parametrization (19) with $v \in S^2$ chosen such that the singularities $x = -v$ and $y = -v$ are far away from the region of integration. For $\mathcal{I}_1$ we choose $v = (0,0,1)$, for $\mathcal{I}_2$ we choose $v = \left(\frac{\sqrt{2}}{2}, 0, -\frac{\sqrt{2}}{2}\right)$ and for $\mathcal{I}_3$ we choose $v = \left(-\frac{\sqrt{2}}{2}, 0, -\frac{\sqrt{2}}{2}\right)$. Therefore, the inner products (17) are given by

$$\langle R\psi_{m,n}, R\psi_{m',n'}\rangle_{L_2(S^2\times S^2)} \;\; = \;\; 2\,\mathcal{I}_1 + 2\,\mathcal{I}_2 + 2\,\mathcal{I}_3\;. \tag{23}$$

This leaves us with one major problem: How to calculate efficiently an integral of type

$$\int e^{i<k,q(\theta,\phi,\alpha,\beta,t)>} f(q(\theta,\phi,\alpha,\beta,t))d\alpha d\beta d\theta d\phi dt \tag{24}$$

with $k = (k_1,\ldots,k_4), q = (q_1,\ldots,q_4)$, $q_i : R^5 \mapsto R$ which is a multidimensional integral of highly oscillatory type.

There are several methods in the literature, such as Fillon-type or Leray-type methods. But applying these method we have to overcome one problem. Usually, in these methods the exponent is linear, while here it is non-linear. An attempt to linearize it could work, but would create a huge number of individual integrals to compute which is difficult to implement.

The way out is to use so-called adaptive multiscale local Fourier bases (see [1], [2] [19]). These bases are generalizations of Malvar-Coifman-Meyer (MCM) wavelets. The basic idea is to use so-called bell functions b_i which provide a partition of unity, i.e. we have a subdivision of our interval $[0, 2\pi]$ into M subintervals I_i where each bell function is defined in three adjacent intervals and given by

$$b_i(x) = \begin{cases} \frac{1}{2}(1 + \sum_{l=0}^{i-1} g_l \sin((n+1)\pi x) & -\frac{1}{2} \leq x \leq \frac{1}{2} \\ \frac{1}{2}(1 + \sum_{l=0}^{i-1} (-1)^l g_l \cos((n+1)\pi x) & \frac{1}{2} \leq x \leq \frac{3}{2} \\ 0 & \text{otherwise} \end{cases}$$

Hereby, g_l are solutions of a linear systems and tabulated in [19]. As remarked before, we have $\sum_{i=1}^{M} b_i(x) = 1$.

These bell functions allow us to introduce our local Fourier basis by

$$u^l_n(\theta,\phi,\alpha,\beta,t) = C^{l_1}_{n_1}(\alpha)C^{l_2}_{n_2}(\beta)C^{l_3}_{n_3}(\theta)C^{l_4}_{n_4}(\phi)C^{l_5}_{n_5}(t)$$

with $C^{l_i}_{n_i}(\cdot) = b_{l_i}(\cdot)\left(\frac{2}{a_{l_i+1}-a_{l_i}}\right)^{1/2} \sin\left(\left(n_i+\frac{1}{2}\right)\pi\frac{\cdot - a_{l_i}}{a_{l_i+1}-a_{l_i}}\right)$.

Application of these LFB's means that we have to calculate the Fourier coefficients

$$\begin{aligned} A_{n,l} &= \int e^{i<k,q(\theta,\phi,\alpha,\beta,t)>} u_n^l(\theta,\phi,\alpha,\beta,t) d\alpha d\beta d\theta d\phi dt \\ B_{n,l} &= \int f(q(\theta,\phi,\alpha,\beta,t)) u_n^l(\theta,\phi,\alpha,\beta,t) d\alpha d\beta d\theta d\phi dt, \end{aligned}$$

separately. The integral is then given by $\sum_{n,l} A_{n,l} B_{n,l}$.

The calculation of the Fourier coefficients can be done either by corrected trapezoidal rule/Richardson interpolation (taking into account the support of the bell functions, but we have to be careful with the number of points we need, see [1], table 2 on page 7) or by FFT (see [19]). Presently, we prefer to use FFT.

Furthermore, we need to study the sparsity condition by Averbuch, et al., for both $B_{n,l}$ and $A_{n,l}$ to determine how many coefficients are really required (see, [1], pg. 14-19). Let us consider our integral in the more shortened form

$$\int e^{i<k,q(\phi_i)>} f(\phi_i) d\phi_1 \dots d\phi_5.$$

For simplification we write just ϕ_i for all our variables. To apply our method we develop our kernel in terms of LFB's:

$$\int e^{i<k,q(\phi_i)>} C_1(\phi_1) \dots C_5(\phi_5) d\phi_1 \dots d\phi_5. \tag{25}$$

Following the same ideas as in [2] we can study the sparsity of this development. The principal condition for the sparsity considerations is that

$$\left| \frac{\partial^{|\mu|}}{\partial \phi_1^{\mu_1} \dots \partial \phi_5^{\mu_5}} q(\phi_1, \dots, \phi_5) \right| \leq C, \tag{26}$$

i.e. the derivatives of order $|\mu|$ are bounded. Let us first remark that our function q satisfies for each subdivision the above condition, but with a constant C which will go to infinity when the total degree for the derivatives goes to infinity, i.e. getting worse with each derivation. Furthermore, we remark that we need at least two points per oscillation, i.e. $N = 10\nu$ (for simplification we consider ν oscillations in all directions otherwise the number of oscillations depends on the direction ϕ_i). That will result in $\sqrt{N} = \sqrt{10}\sqrt{\nu}$ bell functions.

Now, using as rescaling for the bells the maximum frequency, i.e. $\nu = \max_{i=1,2,3} k_i$ we get via linearization for the coefficients (25)

$$\begin{aligned} &\int e^{i<k,q(\phi_i)>} C_1(\phi_1) \dots C_5(\phi_5) d\phi_1 \dots d\phi_5 \\ &\approx e^{i \sum_{l=1}^3 (\sum_{i=1}^3 k_i q_i(\phi^*) - \sum_{i=1}^3 k_i \frac{\partial q_i}{\partial \phi_l}(\phi^*) \phi_l^*)} \int e^{i \sum_{i=1}^3 k_i \frac{\partial q_i}{\partial \phi_1}(\phi^*)) \phi_1} \\ &\times e^{i(\sum_{i=1}^3 k_i \frac{\partial q_i}{\partial \phi_2}(\phi^*)), \phi_2} e^{i(\sum_{i=1}^4 k_i \frac{\partial q_i}{\partial \phi_3}(\phi^*)) \phi_3} e^{i \sum_{i=1}^4 k_i \frac{\partial q_i}{\partial \phi_4}(\phi^*)) \phi_4} \\ &e^{i \sum_{i=1}^4 k_i \frac{\partial q_i}{\partial \phi_5}(\phi^*)) \phi_5} C_1(\phi_1) C_2(\phi_2) C_3(\phi_3) C_4(\phi_4) C_5(\phi_5) d\phi_1 d\phi_2 d\phi_3 d\phi_4 d\phi_5 \end{aligned}$$

We will collect all the exponentials together and denote the residual term (incl. Hessian) of the linearization by $H^{\nu_{k,k'}(\phi_1,\cdots,\phi_5)}$. Using the rescaling of [1] (it corresponds to an independent affine transformation in each variable!) we can view our integral as the Fourier transform of

$$\beta(\phi_1,\cdots,\phi_5) = b(\phi_1)b(\phi_2)b(\phi_3)b(\phi_4)b(\phi_5)e^{iH^{\nu_{k,k'}(\phi_1,\cdots,\phi_5)}}.$$

Now, we prove that there exists a constant K such that

$$\left|H^{\nu}_{k,k'}(\phi_1,\cdots,\phi_5)\right| \leq K$$

and

$$\left|\frac{\partial^{|\mu|}H^{\nu}_{k,k'}}{\partial_{\phi_1^{\mu_1}}\cdots\partial_{\phi_5^{\mu_5}}}(\phi_1,\cdots,\phi_5)\right| \leq \frac{K}{(\sqrt{\nu})^{|\mu|}}.$$

If the first is true then we obtain the second estimate from the rescaling and the fact that at each derivative of q_i a $\sqrt{\nu}$ comes out. With other words the residual (Hessian) has a gradient of order $O\left(\frac{1}{\sqrt{\nu}}\right)$.

This now allows us to get the result of Averbuch, et. al. ([2], pag.18) in our case:

$$|\hat{\beta}(\xi_1,\ldots,\xi_5)| \leq \frac{C_1}{1+\max_i|\xi_i|^{|\mu|}}.$$

What is left is to take a closer look at the first estimate in our case. This estimate follows immediately from estimating the derivatives of the parametrization (c.f. (19))

$$q(x,y,t) = \frac{y+v}{||y+v||}(\cos t + v\sin t)\frac{x+v}{||x+v||}.$$

Here we have to take into account the different nature of x, y on one side and t on the other. By straightforward calculations we get

$$\left\|\frac{\partial^{\mu}q(x,y,t)}{\partial {x_1}^{\mu_1}\ldots\partial {y_1}^{\mu_4}\ldots\partial t^{\mu_7}}\right\| \leq \frac{C_\mu}{\|x+v\|^{\mu_1+\mu_2+\mu_3}\|y+v\|^{\mu_4+\mu_5+\mu_6}}.$$

Let us remark that the denominator is always bounded, but the bound grows with μ, since in the case of (20) we get the estimates $\|y+v\| \geq 1/2$ and $\|x+v\| \geq 1/2$, whereas for (21) and (22) we have $\|y+v\| \geq 2-\sqrt{2}$ and $\|x+v\| \geq 2-\sqrt{2}$.

For the practical implementation we are interested in the second derivatives. Here we can obtain a better estimate than above by directly using a suitable system of spherical coordinates $x = x(\theta,\phi)$ and $y = y(\alpha,\beta)$. The maximum will be reached by the derivatives $\frac{\partial^2 q}{\partial\phi^2}$ and $\frac{\partial^2 q}{\partial\beta^2}$ (c.f. (24)). For these derivatives we get

$$\begin{aligned}\left\|\frac{\partial^2 q}{\partial\phi^2}\right\| \quad \leq \quad & \frac{3|-v_1\cos\theta\cos\phi - v_2\sin\theta\cos\phi + v_3\sin\phi|^2}{||v+x(\theta,\phi)||^4} \\ & + \frac{|v_1\cos\theta\sin\phi + v_2\sin\theta\sin\phi + v_3\cos\phi|}{||v+x(\theta,\phi)||^2} + \\ & + 2\frac{|-v_1\cos\theta\cos\phi - v_2\sin\theta\cos\phi + v_3\sin\phi|}{||v+x(\theta,\phi)||^3} + \frac{1}{||v+x(\theta,\phi)||}\end{aligned}$$

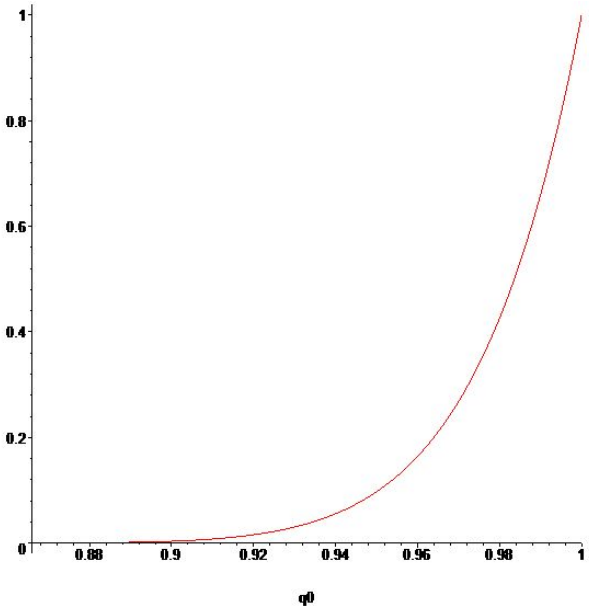

Figure 1: Section of the radial Gabor atom ψ.

and

$$\begin{aligned}\left|\left|\frac{\partial^2 q}{\partial \beta^2}\right|\right| \quad \leq \quad & \frac{3|-v_1\cos\alpha\cos\beta - v_2\sin\alpha\cos\beta + v_3\sin\beta|^2}{||v+y(\alpha,\beta)||^4} \\ & + \frac{|v_1\cos\alpha\sin\beta + v_2\sin\alpha\sin\beta + v_3\cos\beta|}{||v+y(\alpha,\beta)||^2} + \\ & + 2\frac{|-v_1\cos\alpha\cos\beta - v_2\sin\alpha\cos\beta + v_3\sin\beta|}{||v+y(\alpha,\beta)||^3} + \frac{1}{||v+y(\alpha,\beta)||}.\end{aligned}$$

3.4 Christallography and numerical experiments

For the numerical experiments we first have to specify the analyzing Gabor atoms. In the present example we limit ourselves to radial functions over the real axis where ψ is defined by

$$\psi(q) = \cos^6(2.6\arccos(q_0)), \quad \frac{\sqrt{3}}{2} \leq q_0 \leq 1,$$

see Figure 1. If $q = \Lambda(\theta,\alpha,\phi)$, $\theta \in [0, 2\pi[$, $\alpha \in [0,\pi[$ and $\phi \in [0,\pi]$, where Λ is defined as in (6) then the Gabor atom reads as

$$\psi(\theta,\alpha,\phi) = \cos^6(2.6\,\phi), \quad \frac{\pi}{6} \leq \phi \leq \frac{\pi}{2}.$$

The corresponding admissibility constant is

$$C_\psi = 64\pi^5 \int_0^{2\pi}\int_0^{\pi}\int_0^{\pi/2} \frac{|\psi(q(\theta,\alpha,\phi))|^2}{\cos\phi}\, d\phi\, d\alpha\, d\theta \approx 17.54532476\,\pi^7 \approx 52992.$$

The overlapping of the corresponding frame system is as follows. The Gabor atom is defined on the spherical cap

$$U_{\frac{\sqrt{3}}{2}} = \left\{ q \in S^3 : q_0 \geq \frac{\sqrt{3}}{2} \right\}.$$

This cap is centered on the real axis and has a size of $\frac{\pi}{6}$ radians. The spatial grid on S^3 is fixed by the vertices of the 600-cell. This provides us with several advantages. Firstly, the vertices of the 600-cell represent a discrete subgroup of unit quaternions, the binary icosahedral group, a double covering of the icosahedral group. While the group itself is not crystallographic, several crystallographic groups are subgroups of this group, like the cyclic groups generated by the various elements or D_3. Secondly, finer but still quasi-uniform grids can be created starting from this grid by subdivision schemes [21]. As the distance between two neighboring vertices of the 600-cell is $\frac{\pi}{5}$ then the overlapping between two caps is about $\frac{2\pi}{15}$. This gives a ratio of $\frac{4}{5}$ between the overlapping chosen and the maximum overlapping coincident with the distance between two neighboring vertices of the 600-cell. For the frequency grid we prefer the $3-$dimensional grid $3\mathbb{Z}_3 \cup \{(0,0,0)\}$ and for the rotation grid we use the 120 vertices of the 600-cell. For the numerical experiment we choose a (synthetic) example of an ODF with orthorhombic crystal symmetry and triclinic symmetry for the specimen. The ODF itself is simulated in terms of our Gabor system. Based on our grid and the proposed symmetry the vector c representing the coefficients of the ODF has to be sparse. The numerical experiment is now organized as follows. First we simulate data by choosing a vector c that has only zero entries except at labels 1, 46, 47, 48, 49, 50, 51, 120 the entries are one. The related pole figure is visualized in Figure 2. To simulate measurements we derive $R(F^*c)$. To evaluate the reconstruction capacities of the proposed algorithm (12) especially with respect to noisy data, we add in three individual experiments noise with different levels. Proceeding this way, we obtain data with relative errors of 0, 5, and 10 percent. The reconstruction results and the corresponding pole figures are illustrated in Figures 3, 4, 5, 6, 7, and 8.

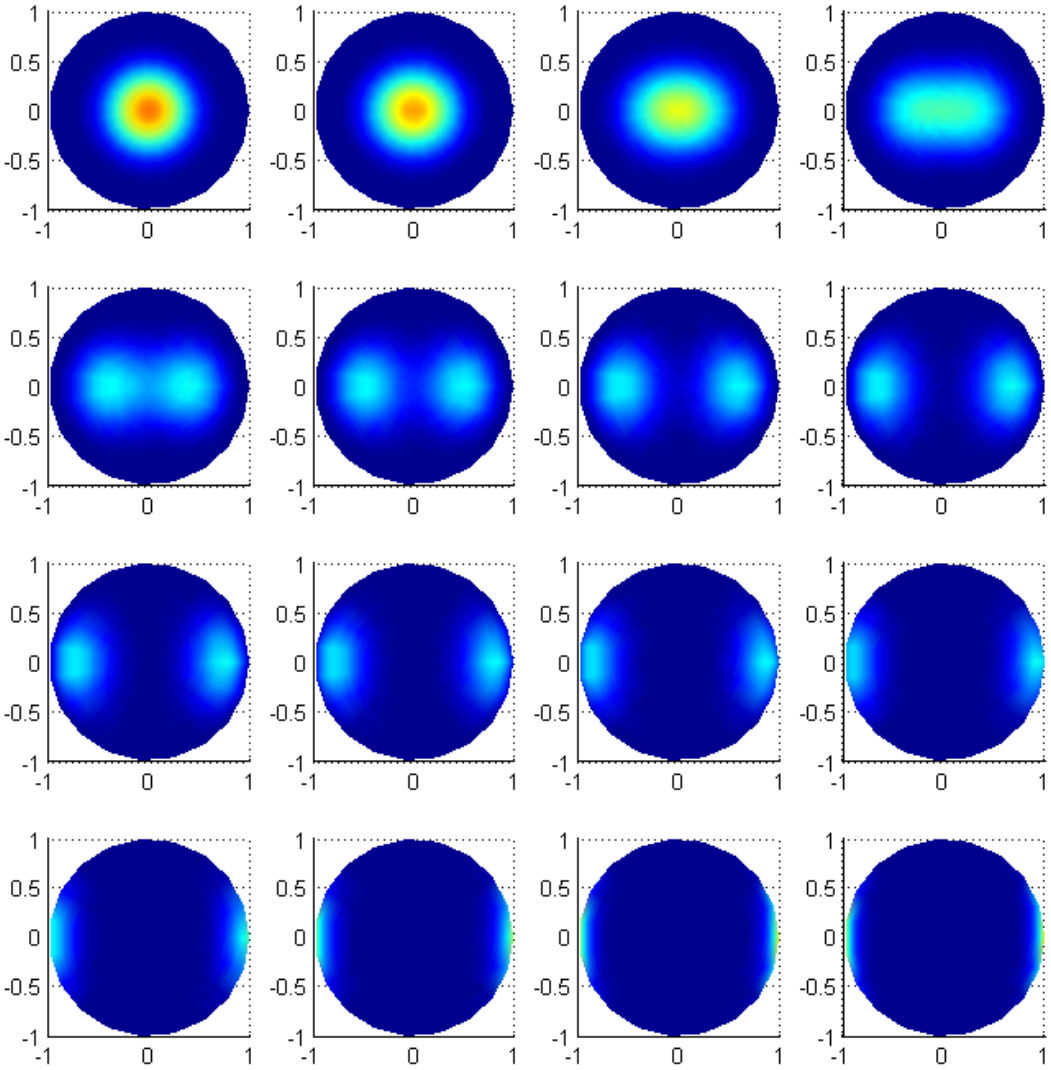

Figure 2: Pole figures for the crystal configuration.

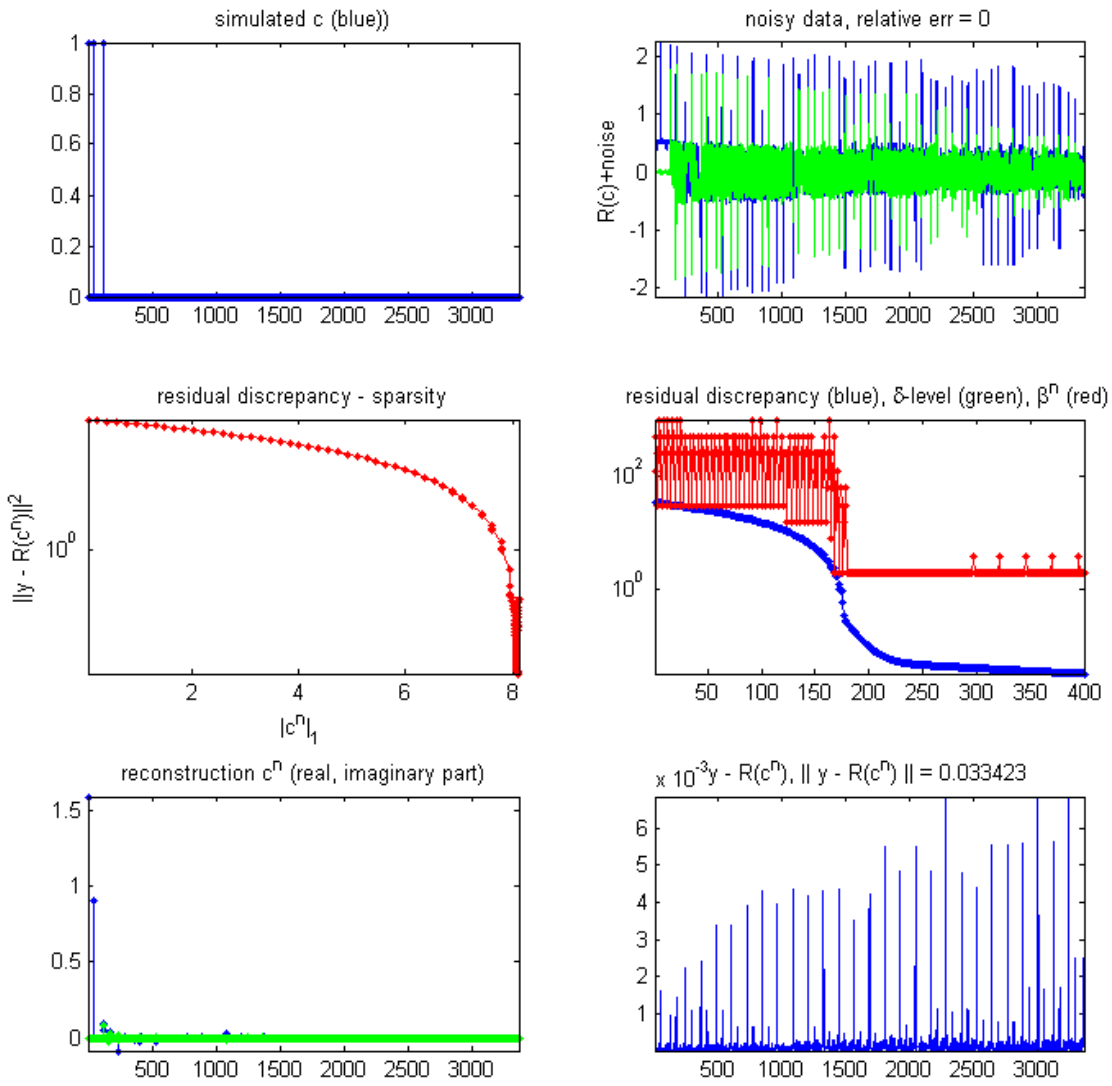

Figure 3: Reconstruction process of iteration (12), relative error of 0.0 percent.

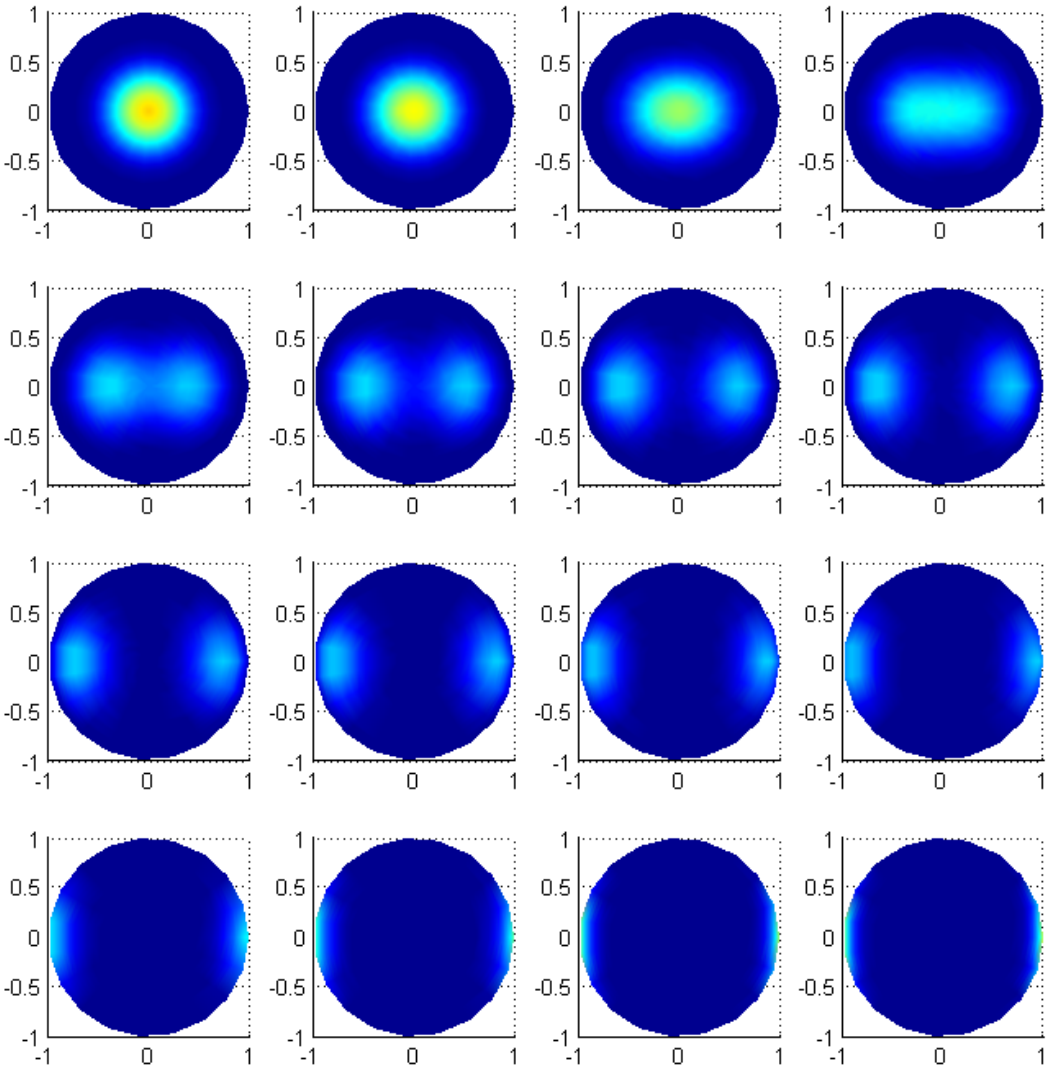

Figure 4: Pole figures for the reconstructed crystal configuration with relative error of 0.0 percent.

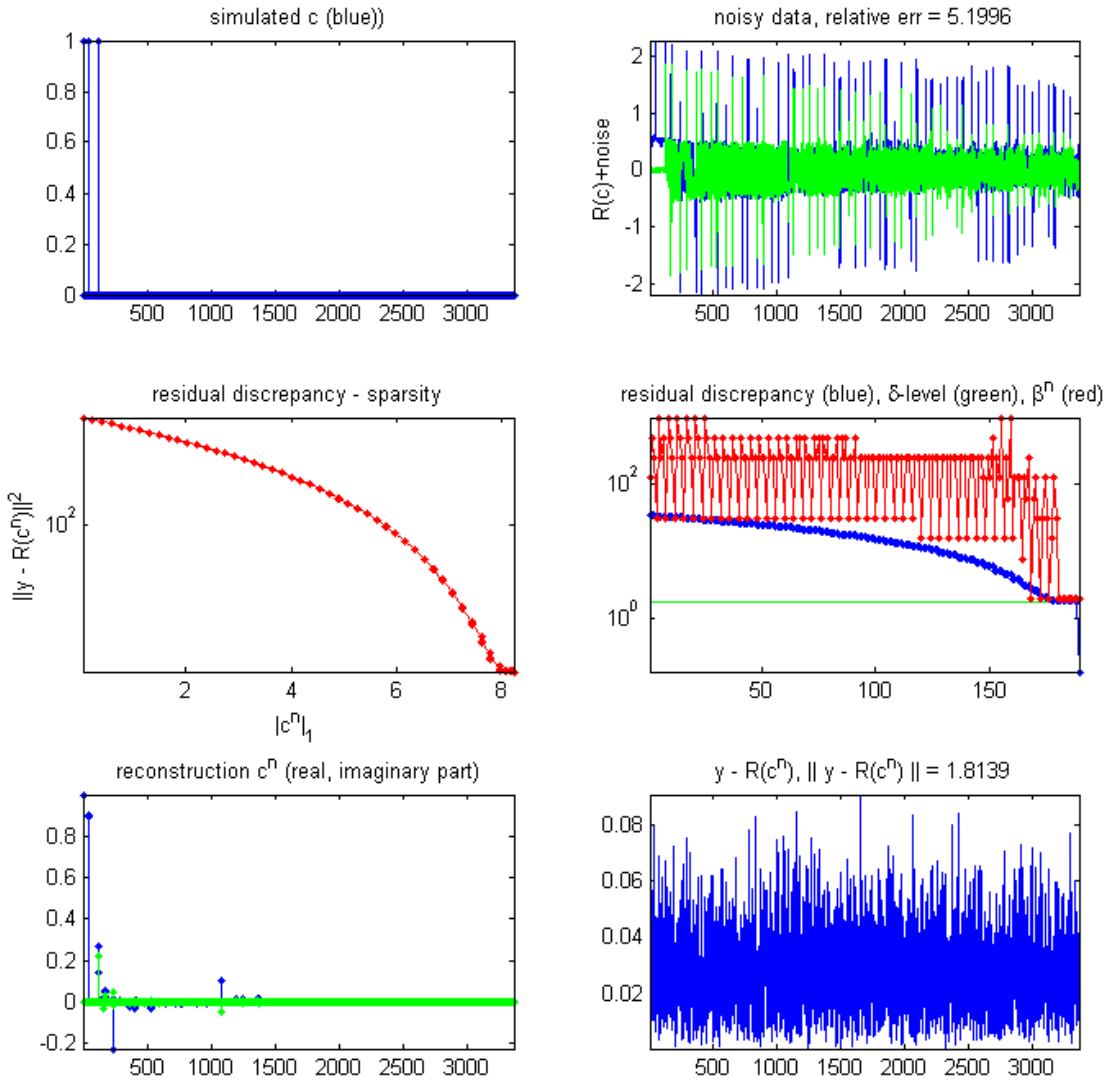

Figure 5: Reconstruction process of iteration (12), relative error of 5.19 percent.

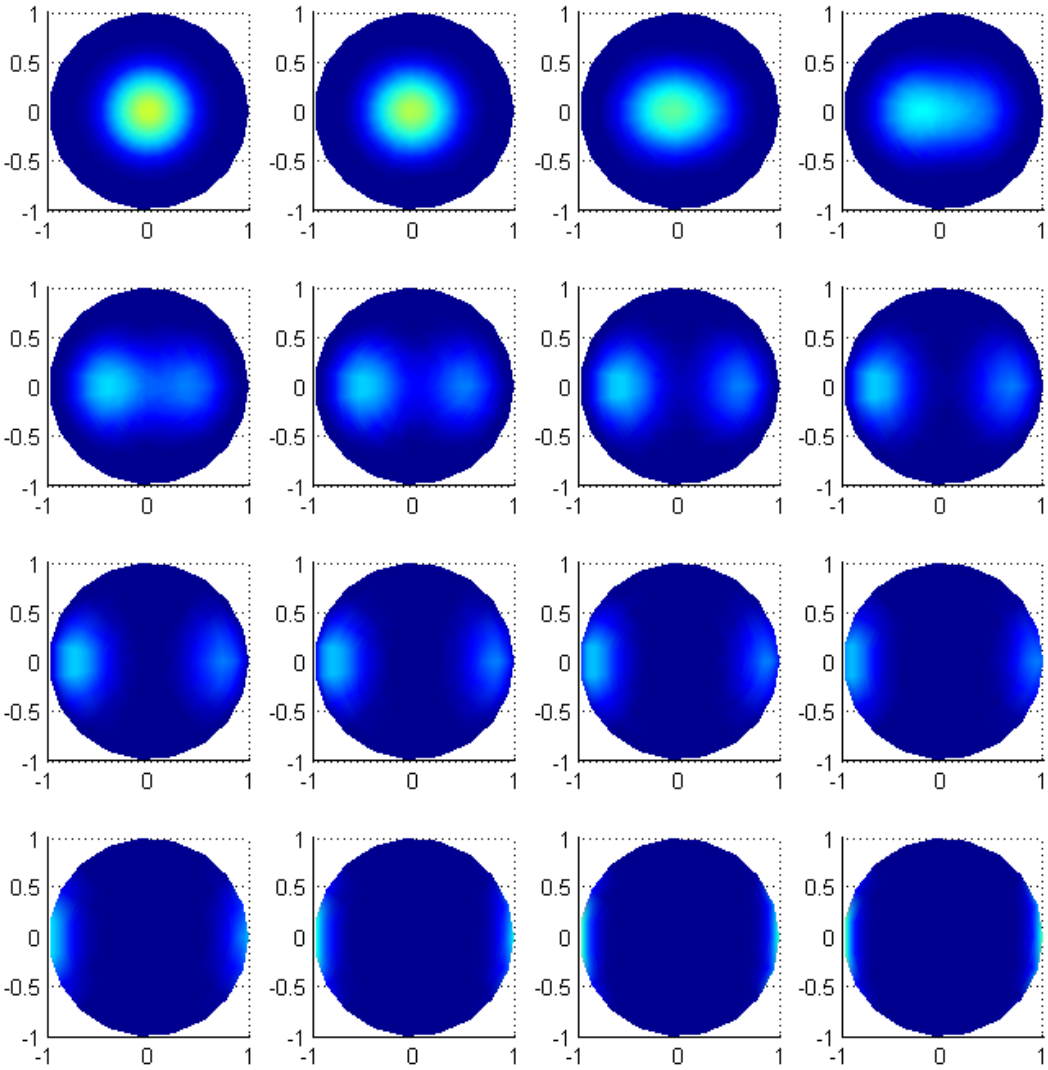

Figure 6: Pole figures for the reconstructed crystal configuration with relative error of 5.19 percent.

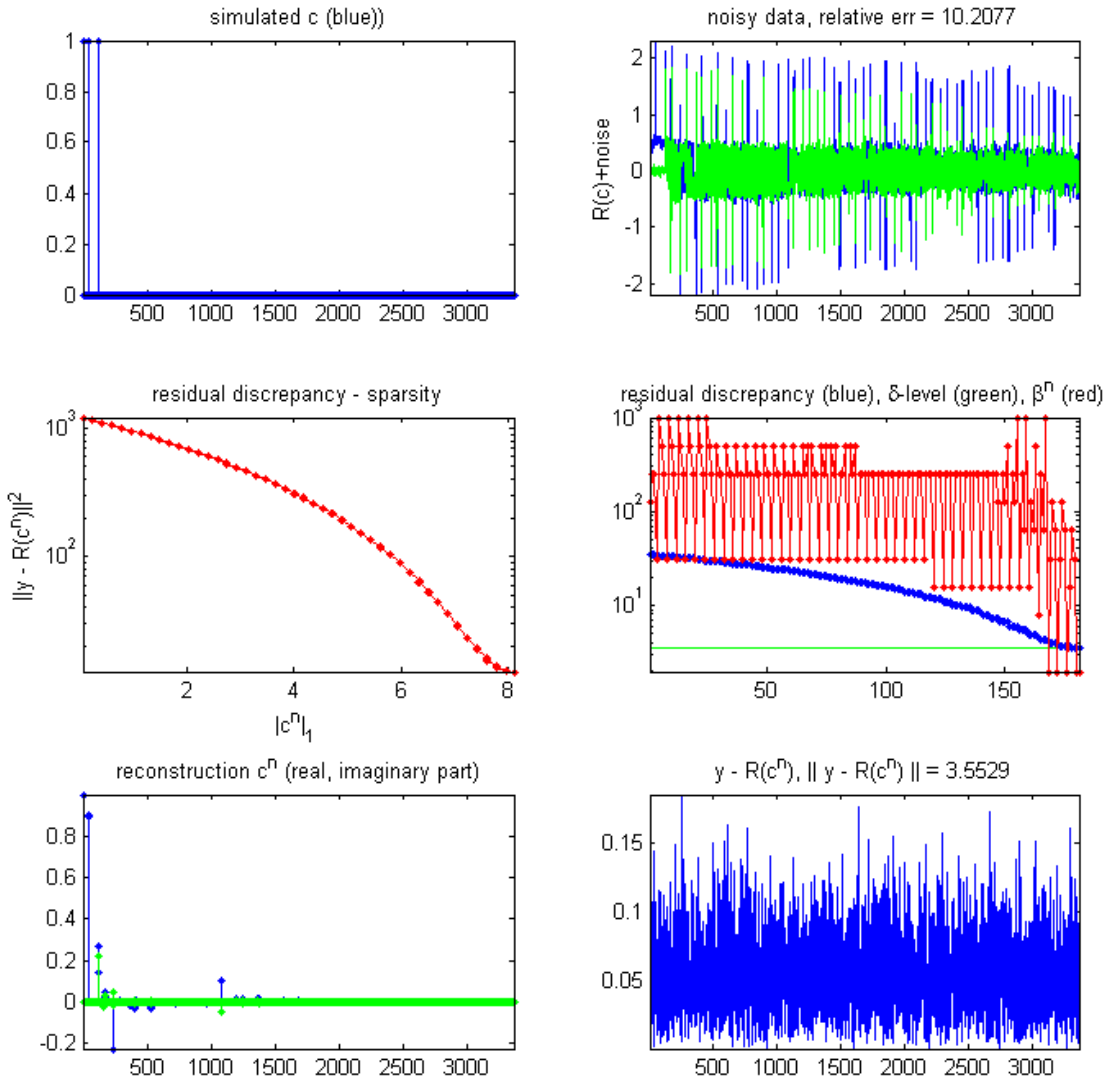

Figure 7: Reconstruction process of iteration (12), relative error of 10.21 percent.

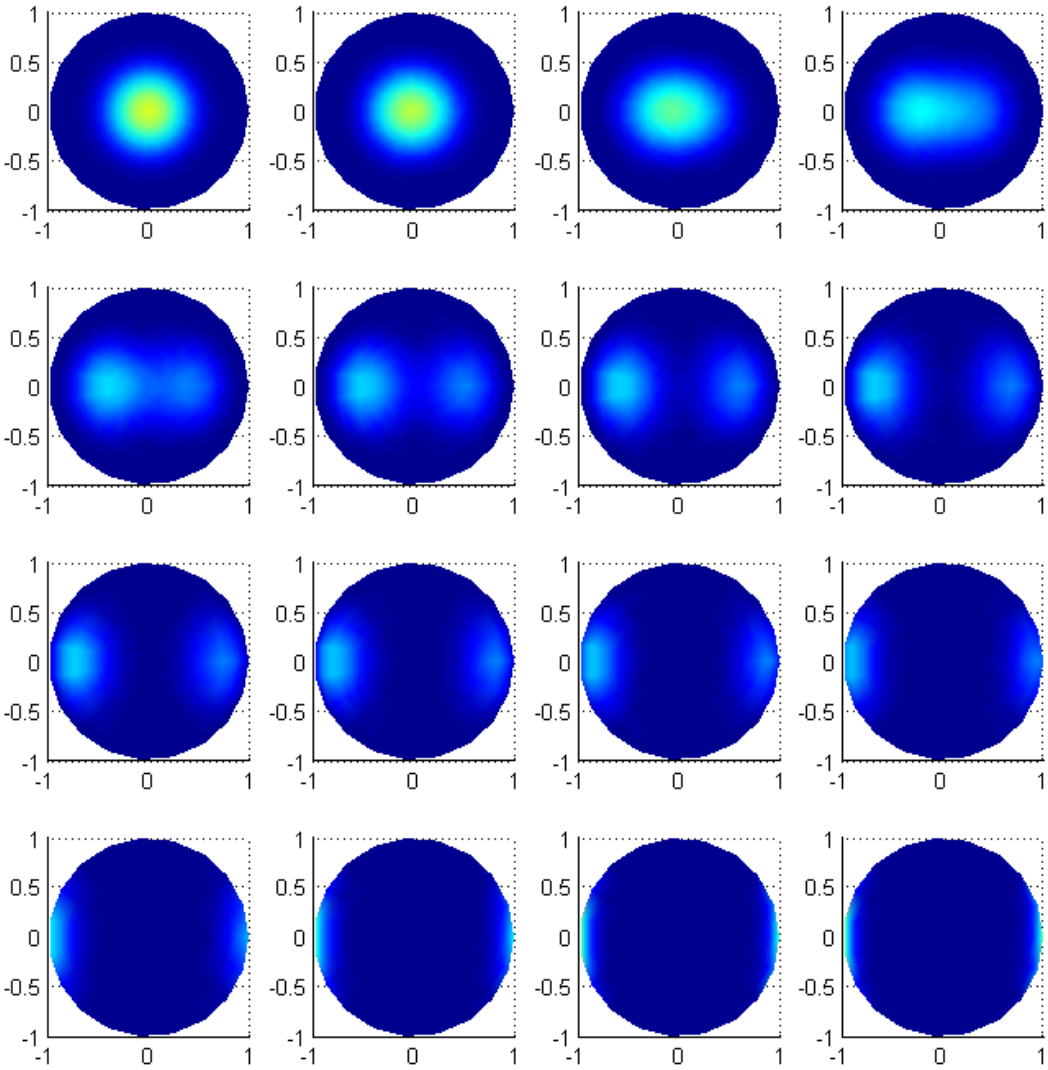

Figure 8: Pole figures for the reconstructed crystal configuration with relative error of 10.21 percent.

A The algebra of quaternions

A.1 Definitions

The algebra of quaternions $\mathbb{H}$ is a four-dimensional real associative division algebra with unit 1 spanned by the elements $\{e_1, e_2, e_3\}$ endowed with the relations

$$e_1^2 = e_2^2 = e_3^2 = -1,$$

$$e_1 e_2 = -e_2 e_1 = e_3, \quad e_2 e_3 = -e_3 e_2 = e_1, \quad e_1 e_3 = -e_3 e_1 = e_2.$$

This algebra is a non-commutative field. The real and imaginary parts of a given quaternion

$$q = x_0 1 + x_1 e_1 + x_2 e_2 + x_3 e_3$$

are defined as $Re(q) = q_0 := x_0$, and $Im(q) = \vec{q} := x_1 e_1 + x_2 e_2 + x_3 e_3$. Therefore, in contrast to complex numbers, $\vec{q}$ is not a real number. We have then natural embeddings of the real numbers and of $\mathbb{R}^3$ into quaternions given by

$$x_0 \in \mathbb{R} \to x_0 1 \in \mathbb{H} \quad \text{and} \quad (x_1, x_2, x_3) \in \mathbb{R}^3 \to x_1 e_1 + x_2 e_2 + x_3 e_3 \in \mathbb{H}.$$

Moreover, we have the identifications $\mathbb{H} \equiv \mathbb{R}^4$, $Im\mathbb{H} \equiv \mathbb{R}^3$, $Re\mathbb{H} \equiv \mathbb{R}$, where $Im\mathbb{H}$ is the three dimensional space of imaginary quaternions, and $\mathbb{H} = \mathbb{R} \oplus \mathbb{R}^3$.

There is a suitable conjugation on $\mathbb{H}$, given by

$$q = x_0 + \vec{q} \to \overline{q} = x_0 - \vec{q}$$

and satisfying to the involution property $\overline{qp} = \overline{p}\,\overline{q}$. The Euclidean scalar product is defined on $\mathbb{H} = \mathbb{R}^4$ by $< q, p >= Re(q\overline{p}) = \frac{1}{2}(q\overline{p} + p\overline{q})$ and the corresponding norm $\|q\|^2 =< q, q >$ verifies $\|qp\| = \|q\|\ \|p\|$. The quaternionic multiplication can be expressed in terms of the usual scalar and vector product on $Im\mathbb{H} \equiv \mathbb{R}^3$ by

$$qp = (q_0 + \vec{q})(p_0 + \vec{p}) = q_0 p_0 - \vec{q} \cdot \vec{p} + q_0 \vec{p} + p_0 \vec{q} + \vec{q} \times \vec{p}.$$

A.2 Rotations in $\mathbb{R}^3$ and $\mathbb{R}^4$

The set of unitary quaternions $S^3 = \{q \in \mathbb{H}, \|q\| = 1\}$ is a group under multiplication. It can be interpreted also as a group of linear maps $p \in \mathbb{H} \to qp$ which preserves the ($\mathbb{H}$-valued) hermitian product $p|q = \overline{p}q$ and it is usually called the symplectic group $Sp(1)$. The action of $Sp(1)$ on $\mathbb{H}$ given by $\hat{\rho}(q) : \mathbb{H} \to \mathbb{H}$, $\hat{\rho}(q)p = qp\overline{q}$, $\quad q \in Sp(1)$ preserves the Euclidean scalar product on $\mathbb{R}^4$, it stabilizes $\mathbb{R} \subset \mathbb{H}$ and its orthogonal complement $Im\mathbb{H}$. Also, we define the automorphic groups $SO(3)$ and $SO(4)$ as

$$SO(3) = \{T \in Aut(\mathbb{H}) : (T\vec{q}) \cdot (T\vec{p}) = \vec{q} \cdot \vec{p},\ \vec{q}, \vec{p} \in \mathbb{R}^3 \equiv Im\mathbb{H}\},$$

and

$$SO(4) = \{Q \in Aut(\mathbb{H}) :< Qq, Qp >=< q, p >, q, p \in \mathbb{H}\}.$$

The restriction of the action of the group $Sp(1)$ on $\mathbb{R}^3 = Im\mathbb{H}$ is a representation of $Sp(1)$ by rotations and it induces a homomorphism $\hat{\rho} : Sp(1) \to SO(3)$ which can be shown to be the universal covering of the group $SO(3) \simeq Sp(1)/\mathbb{Z}_2$. Hence $Sp(1)$ is also isomorphic to $Spin(3)$.

Finally, the map $\rho : Sp(1) \times Sp(1) \to SO(4)$, $(u, v) \to \rho(u, v)(q) = uq\overline{v}$ preserves the Euclidean norm in $\mathbb{R}^4$, that is,

$$\|uq\overline{v}\|^2 = Re(uq\overline{v}\ \overline{uq\overline{v}}) = Re(uq\overline{v}\ v\overline{qu}) = Re(q\overline{q}) = \|q\|^2.$$

Therefore, we have a homomorphism of $Sp(1) \times Sp(1)$. Moreover, it can be shown that ρ defines a two-fold covering of the special orthogonal group $SO(4)$ and so, we have $Spin(4) \equiv Sp(1) \times Sp(1)$.

Acknowledgements

The research of P. Cerejeiras, M. Ferreira, and U. Kähler was (partially) supported by *Unidade de Investigação Matemática e Aplicações* of Universidade de Aveiro, through *Programa Operacional "Ciência, Tecnologia, Inovação"* (POCTI) of the *Fundação para a Ciência e a Tecnologia (FCT)*, cofinanced by the European Community fund FEDER. G. Teschke gratefully acknowledges support by DAAD Grant D/07/13641.

References

[1] A. Averbuch, E. Braverman, R. Coifman, M. Israeli, and A. Sidi, Efficient Computation of Oscillatory Integrals via Adaptive Multiscale Local Fourier Bases, Applied and Computational Harmonic Analysis, **9** (2000), no. 1, 19-53.

[2] A. Averbuch, E. Braverman, R. Coifman, and M. Israeli, On efficient computation of multidimensional oscillatory integrals with local Fourier bases, J. of Nonlinear Analysis: Series A Theory and Methods, **47** (2001), 3491-3502.

[3] S. Bernstein, and H. Schaeben, *A one-dimensional Radon transform on SO(3) and its application to texture goniometry*, Math. Methods Appl. Sci., **28** (2005), 126989.

[4] K.G. v.d. Boogaart, R. Hielscher, J. Prestin and H. Schaeben, *Kernel-based methods for inversion of the radon transform on SO(3) and their applications to texture analysis*, J. Comput. Appl. Math. **199** (2007), 122-40.

[5] H.J. Bunge, *Texture Analysis in Material Science* (London: Butterworths), 1982.

[6] P. Cerejeiras, H. Schaeben, and F. Sommen *The spherical x-ray transform*, Math. Methods Appl. Sci., **25** (2002), 1493507.

[7] S. Dahlke, G. Steidl and G. Teschke, *Frames and Coorbit Theory on Homogeneous Spaces with a Special Guidance on the Sphere*, Special Issue: Analysis on the Sphere, Journal of Fourier Analysis and Applications, **13(4)**, (2007), 387-403.

[8] S. Dahlke, G. Steidl, and G. Teschke, *Weighted Coorbit Spaces and Banach Frames on Homogeneous Spaces* J. of Fourier Anal. Appl. **10(5)** (2004), 507-539.

[9] I. Daubechies, M. Fornasier, and I. Loris. Accelerated projected gradient methods for linear inverse problems with sparsity constraints. *J. Fourier Anal. Appl.*, to appear (2008).

[10] I. Daubechies, M. Defrise, and C. DeMol. An iterative thresholding algorithm for linear inverse problems with a sparsity constraint. *Comm. Pure Appl. Math*, 57 (2004), 1413–1541.

[11] I. Daubechies and G. Teschke. *Variational image restoration by means of wavelets: simultaneous decomposition, deblurring and denoising*, Applied and Computational Harmonic Analysis, **19(1)** (2005), 1-16.

[12] I. Daubechies, G. Teschke and L. Vese. *Iteratively solving linear inverse problems with general convex constraints*, Inverse Problems and Imaging, **1(1)** (2007), 29-46.

[13] I. Daubechies, G. Teschke and L. Vese, *On some iterative concepts for image restoration*, Advances in Imaging and Electron Physics, **150** (2008), 1-51.

[14] R. Delanghe, F. Sommen, and V. Souček, *Clifford analysis and spinor-valued functions: a function theory for the Dirac operator*, Math. and its Appl. **53**, Kluwer Acad. Publ., Dordrecht, 1992.

[15] R. Hielscher, *The Radon transform on the rotation group inversion and application to texture analysis* Dissertation, Department of Geosciences, University of Technology Freiberg (2007). https://fridolin.tufreiberg.de/archiv/html/MathematikHielscherRalf361401.html

[16] R. Hielscher, D. Potts, J. Prestin, H. Schaeben, and M. Schmalz. *The Radon transform on $SO(3)$: a Fourier slice theorem and numerical inversion*, Invers. Prob. **24** (2008), doi:10.1088/0266-5611/24/2/025011.

[17] U.F. Kocks, C.N. Tomé, H.R. Wenk and H. Mecking, *Texture and Anisotropy* (Cambridge: Cambridge University Press), 1998.

[18] S. Matthies, G. Vinel and K. Helmig, *Standard Distributions in Texture Analysis* vol 1 (Berlin: Akademie- Verlag), 1987.

[19] G. Matviyenko, Optimized Local Trigonometric Bases, Applied and Computational Harmonic Analysis, **3** (1996), 301-323.

[20] L. Meister, H. Schaeben, *A concise quaternion geometry of rotations*, MMAS **28** (2004), 101126.

[21] G. Nawratil and H. Pottmann, *Subdivision Schemes for the fair Discretization of the Spherical Motion Group*, Technical Report, Vienna University of Technology, June 2007.

[22] D. I. Nikolayev, and H. Schaeben, *Characteristics of the ultra-hyperbolic differential equation governing pole density functions*, Inverse Probl., **15** (1999), 160319.

[23] R. Ramlau, G. Teschke and M. Zhariy, *A Compressive Landweber Iteration for Solving Ill-posed Inverse Problems*, Inverse Probl., **24(6)** (2008), 065013.

[24] V. Randle and O. Engler, *Introduction to Texture Analysis Macrotexture: Microtexture and Orientation Mapping* (London: Gordon and Breach), 2000.

[25] H. Schaeben and K.G. v. d. Boogaart, *Spherical harmonics in texture analysis*, Tectonophysics **370** (2003), 253-68.

[26] G. Teschke. *Multi-Frame Representations in Linear Inverse Problems with Mixed Multi-Constraints*, Applied and Computational Harmonic Analysis, **22** (2007), 43-60.

[27] G. Teschke and C. Borries *Accelerated Projected Steepest Descent Method for Nonlinear Inverse Problems with Sparsity Constraints*, Inverse Problems **26** (2010), 025007.

[28] Torrésani, B., *Phase space decompositions: Local Fourier analysis on spheres*, preprint CPT-93/P.2878, Marseille (1993); Signal Proc. **43** (1995), 341-346.

Preprint Series DFG-SPP 1324

http://www.dfg-spp1324.de

Reports

[1] R. Ramlau, G. Teschke, and M. Zhariy. A Compressive Landweber Iteration for Solving Ill-Posed Inverse Problems. Preprint 1, DFG-SPP 1324, September 2008.

[2] G. Plonka. The Easy Path Wavelet Transform: A New Adaptive Wavelet Transform for Sparse Representation of Two-dimensional Data. Preprint 2, DFG-SPP 1324, September 2008.

[3] E. Novak and H. Woźniakowski. Optimal Order of Convergence and (In-) Tractability of Multivariate Approximation of Smooth Functions. Preprint 3, DFG-SPP 1324, October 2008.

[4] M. Espig, L. Grasedyck, and W. Hackbusch. Black Box Low Tensor Rank Approximation Using Fibre-Crosses. Preprint 4, DFG-SPP 1324, October 2008.

[5] T. Bonesky, S. Dahlke, P. Maass, and T. Raasch. Adaptive Wavelet Methods and Sparsity Reconstruction for Inverse Heat Conduction Problems. Preprint 5, DFG-SPP 1324, January 2009.

[6] E. Novak and H. Woźniakowski. Approximation of Infinitely Differentiable Multivariate Functions Is Intractable. Preprint 6, DFG-SPP 1324, January 2009.

[7] J. Ma and G. Plonka. A Review of Curvelets and Recent Applications. Preprint 7, DFG-SPP 1324, February 2009.

[8] L. Denis, D. A. Lorenz, and D. Trede. Greedy Solution of Ill-Posed Problems: Error Bounds and Exact Inversion. Preprint 8, DFG-SPP 1324, April 2009.

[9] U. Friedrich. A Two Parameter Generalization of Lions' Nonoverlapping Domain Decomposition Method for Linear Elliptic PDEs. Preprint 9, DFG-SPP 1324, April 2009.

[10] K. Bredies and D. A. Lorenz. Minimization of Non-smooth, Non-convex Functionals by Iterative Thresholding. Preprint 10, DFG-SPP 1324, April 2009.

[11] K. Bredies and D. A. Lorenz. Regularization with Non-convex Separable Constraints. Preprint 11, DFG-SPP 1324, April 2009.

[12] M. Döhler, S. Kunis, and D. Potts. Nonequispaced Hyperbolic Cross Fast Fourier Transform. Preprint 12, DFG-SPP 1324, April 2009.

[13] C. Bender. Dual Pricing of Multi-Exercise Options under Volume Constraints. Preprint 13, DFG-SPP 1324, April 2009.

[14] T. Müller-Gronbach and K. Ritter. Variable Subspace Sampling and Multi-level Algorithms. Preprint 14, DFG-SPP 1324, May 2009.

[15] G. Plonka, S. Tenorth, and A. Iske. Optimally Sparse Image Representation by the Easy Path Wavelet Transform. Preprint 15, DFG-SPP 1324, May 2009.

[16] S. Dahlke, E. Novak, and W. Sickel. Optimal Approximation of Elliptic Problems by Linear and Nonlinear Mappings IV: Errors in L_2 and Other Norms. Preprint 16, DFG-SPP 1324, June 2009.

[17] B. Jin, T. Khan, P. Maass, and M. Pidcock. Function Spaces and Optimal Currents in Impedance Tomography. Preprint 17, DFG-SPP 1324, June 2009.

[18] G. Plonka and J. Ma. Curvelet-Wavelet Regularized Split Bregman Iteration for Compressed Sensing. Preprint 18, DFG-SPP 1324, June 2009.

[19] G. Teschke and C. Borries. Accelerated Projected Steepest Descent Method for Nonlinear Inverse Problems with Sparsity Constraints. Preprint 19, DFG-SPP 1324, July 2009.

[20] L. Grasedyck. Hierarchical Singular Value Decomposition of Tensors. Preprint 20, DFG-SPP 1324, July 2009.

[21] D. Rudolf. Error Bounds for Computing the Expectation by Markov Chain Monte Carlo. Preprint 21, DFG-SPP 1324, July 2009.

[22] M. Hansen and W. Sickel. Best m-term Approximation and Lizorkin-Triebel Spaces. Preprint 22, DFG-SPP 1324, August 2009.

[23] F.J. Hickernell, T. Müller-Gronbach, B. Niu, and K. Ritter. Multi-level Monte Carlo Algorithms for Infinite-dimensional Integration on $\mathbb{R}^{\mathbb{N}}$. Preprint 23, DFG-SPP 1324, August 2009.

[24] S. Dereich and F. Heidenreich. A Multilevel Monte Carlo Algorithm for Lévy Driven Stochastic Differential Equations. Preprint 24, DFG-SPP 1324, August 2009.

[25] S. Dahlke, M. Fornasier, and T. Raasch. Multilevel Preconditioning for Adaptive Sparse Optimization. Preprint 25, DFG-SPP 1324, August 2009.

[26] S. Dereich. Multilevel Monte Carlo Algorithms for Lévy-driven SDEs with Gaussian Correction. Preprint 26, DFG-SPP 1324, August 2009.

[27] G. Plonka, S. Tenorth, and D. Roşca. A New Hybrid Method for Image Approximation using the Easy Path Wavelet Transform. Preprint 27, DFG-SPP 1324, October 2009.

[28] O. Koch and C. Lubich. Dynamical Low-rank Approximation of Tensors. Preprint 28, DFG-SPP 1324, November 2009.

[29] E. Faou, V. Gradinaru, and C. Lubich. Computing Semi-classical Quantum Dynamics with Hagedorn Wavepackets. Preprint 29, DFG-SPP 1324, November 2009.

[30] D. Conte and C. Lubich. An Error Analysis of the Multi-configuration Time-dependent Hartree Method of Quantum Dynamics. Preprint 30, DFG-SPP 1324, November 2009.

[31] C. E. Powell and E. Ullmann. Preconditioning Stochastic Galerkin Saddle Point Problems. Preprint 31, DFG-SPP 1324, November 2009.

[32] O. G. Ernst and E. Ullmann. Stochastic Galerkin Matrices. Preprint 32, DFG-SPP 1324, November 2009.

[33] F. Lindner and R. L. Schilling. Weak Order for the Discretization of the Stochastic Heat Equation Driven by Impulsive Noise. Preprint 33, DFG-SPP 1324, November 2009.

[34] L. Kämmerer and S. Kunis. On the Stability of the Hyperbolic Cross Discrete Fourier Transform. Preprint 34, DFG-SPP 1324, December 2009.

[35] P. Cerejeiras, M. Ferreira, U. Kähler, and G. Teschke. Inversion of the noisy Radon transform on $SO(3)$ by Gabor frames and sparse recovery principles. Preprint 35, DFG-SPP 1324, December 2009.